Comparative study of the decays $B\to(K,K^*)l^+l^-$ in the standard model and supersymmetric theories

A. Ali,[1,*] Patricia Ball,[2,†] L. T. Handoko,[1,3,‡] and G. Hiller[4,§]
[1]*Deutsches Elektronen-Synchrotron DESY, Notkestr. 85, D–22607 Hamburg, Germany*
[2]*CERN/TH, CH–1211 Geneva 23, Switzerland*
[3]*Laboratory for Theoretical Physics and Mathematics, LIPI, Kom. Puspitek Serpong P3FT–LIPI, Tangerang 15310, Indonesia*
[4]*INFN, Laboratori Nazionali di Frascati, P.O. Box 13, I–00044 Frascati, Italy*
(Received 5 October 1999; published 8 March 2000)

Using improved theoretical calculations of the decay form factors in the light cone QCD sum rule approach, we investigate the decay rates, dilepton invariant mass spectra and the forward-backward (FB) asymmetry in the decays $B\to(K,K^*)l^+l^-$ ($l^\pm=e^\pm,\mu^\pm,\tau^\pm$) in the standard model (SM) and a number of popular variants of the supersymmetric (SUSY) models. Theoretical precision on the differential decay rates and FB asymmetry is estimated in these theories taking into account various parametric uncertainties. We show that existing data on $B\to X_s\gamma$ and the experimental upper limit on the branching ratio $\mathcal{B}(B\to K^*\mu^+\mu^-)$ provide interesting bounds on the coefficients of the underlying effective theory. We argue that the FB asymmetry in $B\to K^*l^+l^-$ constitutes a precision test of the SM and its measurement in forthcoming experiments may reveal new physics. In particular, the presently allowed large-tan β solutions in SUGRA models, as well as more general flavor-violating SUSY models, yield FB asymmetries which are characteristically different from the corresponding ones in the SM.

PACS number(s): 13.20.He, 13.25.Hw

I. INTRODUCTION

The flavor-changing-neutral-current (FCNC) transitions $B\to(X_s,X_d)\gamma$ and $B\to(X_s,X_d)l^+l^-$, with X_s (X_d) being hadrons with overall strangeness $S=\pm1$ ($S=0$), provide potentially stringent tests of the standard model (SM) in flavor physics. FCNC transitions are forbidden in the SM Lagrangian and are induced by the Glashow-Iliopoulos-Maiani (GIM) amplitudes [1] at the loop level, which makes their effective strengths small. In addition, these transitions may also be parametrically suppressed in the SM due to their dependence on the weak mixing angles of the quark-flavor rotation matrix — the Cabibbo-Kobayashi-Maskawa (CKM) matrix VCKM [2]. These two circumstances make the FCNC decays relatively rare and hence vulnerable to the presence of new physics. In the context of the SM, the potential interest in rare B decays is that they would provide a quantitative determination of the quark-flavor rotation matrix, in particular the matrix elements V_{tb}, V_{td} and V_{ts} [3–6]. A beginning in that direction has already been made by the measurement of the branching ratio $\mathcal{B}(B\to X_s\gamma)$ [7,8], yielding $|V_{ts}V_{tb}^*|=0.035\pm0.004$ [9], in agreement with the expectations based on the CKM unitarity [10]. Since complementary information will also be available from the B_s^0-$\overline{B_s^0}$- and B_d^0-$\overline{B_d^0}$-mixing induced mass differences ΔM_s and ΔM_d, respectively, and from a number of rare kaon decays [11], the parameters of the CKM matrix, which are already fairly constrained in the SM [12–14], will be multiply determined. This will result either in precise determination of the SM parameters in the flavor sector, comparable to the precision of the electroweak parameters of the SM [15], or, more optimistically, in the discovery of new physics. Thus, FCNC processes are potentially effective tools in searching for new physics, with the supersymmetric theories receiving special attention in this context [12,16–24].

Inclusive decay rates and distributions are relatively robust theoretically, making them well-suited to search for new physics which may result in distortions of the SM distributions. Concerning rare B decays, we recall that the shape of the photon energy spectra in the radiative decays $B\to(X_s,X_d)\gamma$ depends on the underlying physics. However, deviations from the SM-based normalized photon-energy distributions are expected only for the low-to-intermediate photon energies, where the individual contributions from the various operators in the underlying effective theory are comparable. Measuring the low-E_γ spectrum is, however, a formidable task in the present experimental setup. More promising from the point of view of observing new-physics-induced distortions in the distributions are the decays $B\to(X_s,X_d)l^+l^-$, which provide the possibility of measuring Dalitz-distributions in a number of variables, which in turn could be used to determine the coefficients of the effective vertices in the underlying theory [17]. This program is somewhat handicapped by the fact that heavy quark expansion in $1/m_b$ breaks down near the endpoints of the spectra [25,26], near the $c\bar{c}$ threshold and in the resonant region. Thus, a certain amount of modeling is unavoidable for the complete phenomenological profile of the decays $B\to X_sl^+l^-$. A number of studies has been undertaken to assess the nonperturbative effects [25,27–32], allowing one to define lim-

*Email address: ali@x4u2.desy.de
†Email address: Patricia.Ball@cern.ch
‡Email address: handoko@mail.desy.de
§Email address: Gudrun.Hiller@lnf.infn.it; Address since Oct.1, 1999: SLAC, P.O.Box 4349, Stanford, CA 94309.

ited kinematic regions where the short-distance physics in the SM and alternative theories can be quantitatively studied.

While the inclusive rare decays discussed above are theoretically cleaner than exclusive decays, which require additionally the knowledge of form factors, they are also more difficult to measure. Present best limits from the CLEO Collaboration on $B\to X_s\mu^+\mu^-$ and $B\to X_s e^+e^-$ [33] decays are typically an order of magnitude larger than the corresponding SM-based estimates [25]. Moreover, inclusive rare decays are a challange for experiments operating at hadron machines. However, it is encouraging that the FCNC exclusive semileptonic decays, in particular the $B\to(K,K^*)\mu^+\mu^-$ modes, are accessible to a wider variety of experiments. As we will argue quantitatively in this paper, some of the present experimental bounds on these (and related e^+e^- modes) [34,35] are already quite stringent. With the advent of the Fermilab booster, DESY HERA-B, experiments at the CERN Large Hadron Collider (LHC), and also the ongoing experiments at CLEO and the *B* factories, the decays of interest $B\to(K,K^*)l^+l^-$ will be precisely measured. It is therefore worthwhile to return to a comparative study of these decays in the SM and some candidate theories of physics beyond the SM to ascertain if these modes could be meaningfully used for searches of beyond-the-SM physics.

In the context of the SM, exclusive FCNC semileptonic *B* decays have been studied in a number of papers [36–44] with varying degrees of theoretical rigor and emphasis. The main purpose of this paper is twofold: First, we would like to report on an improved calculation of the decay form factors using the technique of the light cone QCD sum rules (LCSR) [45,46]. Early studies of exclusive *B* decays in the LCSR approach were restricted to contributions of leading twist and did not take into account radiative corrections (see Refs. [47,48] for a review and references to original publications). In the present paper, we use the results of [49] for vector form factors, which include next to leading order (NLO) radiative corrections and higher twist corrections up to twist 4 [50,51]. For $B\to K$ form factors we improve on the results obtained in [52] by including the twist 4 mass correction terms calculated in [53]. Second, we apply this technology to the SM and some popular variants of the SUSY models to determine the phenomenological profiles of the decays $B\to(K,K^*)l^+l^-$ in these scenarios. For the latter, we choose minimal- and non-minimal SUGRA models, minimal flavor violating (MFV) supersymmetric model, and a general flavor-violating supersymmetric framework, studied in the mass insertion approximation (MIA). While all these models have been studied quite extensively in the literature for the inclusive decays $B\to X_s\gamma$ and $B\to X_s l^+l^-$ [16–24], we are not aware of corresponding studies for the exclusive decays. We strive to fill this gap in this paper.

With our goals clearly stated, we turn to the main issues in the inclusive and exclusive rare *B* decays. Using the language of effective theories and restricting ourselves to the SM and SUSY, the short-distance contributions in the decays $B\to X_s\gamma$ and $B\to X_s l^+l^-$, and the exclusive decays of interest to us, are determined by three coefficients, called $C_7^{\rm eff}$, C_9 and C_{10} [54,55].[1] Of these, $|C_7^{\rm eff}|$ — the modulus of the effective coefficient of the electromagnetic penguin operator — is bounded by the present experimental measurements of the $B\to X_s\gamma$ branching ratio [7,8]. Using the 95% C.L. upper and lower bounds from the updated CLEO measurements [7],

$$2.0\times10^{-4}<\mathcal{B}(B\to X_s\gamma)<4.5\times10^{-4}, \tag{1.1}$$

one gets in the next-to-leading precision the bounds:

$$0.28\leqslant|C_7^{\rm eff}(m_B)|\leqslant0.41. \tag{1.2}$$

The magnitude of $C_7^{\rm eff}(m_B)$ in the SM [56] is well within the CLEO bounds but there is no experimental information on the phase of $C_7^{\rm eff}(m_B)$. It is imperative to determine this sign experimentally, as it is model-dependent. In particular, in supergravity- (SUGRA-)type theories, both positive and negative-valued solutions for $C_7^{\rm eff}(m_B)$ are allowed in different SUSY-parameter regions.

Despite the present lack of direct information on the sign of $C_7^{\rm eff}(m_B)$, the bound in Eq. (1.2) is quite stringent and effectively limits possible new-physics effects due to the inherent correlations among the branching ratio $\mathcal{B}(B\to X_s\gamma)$ and other observable quantities such as the B^0-$\overline{B^0}$ mixing, ϵ_K and the mass of the CP-even Higgs boson, m_h. In particular, in the context of the minimal SUGRA (MSUGRA) models, present data on $\mathcal{B}(B\to X_s\gamma)$ [7,8] and lower bounds on m_h [57] do not allow the effective coefficient $C_7^{\rm eff}(m_B)$ to have a positive sign [22]. However, relaxing the grand unified theory (GUT) mass constraints on the parameters of the scalar superpotential, large-tanβ solutions exist, which are compatible with all present experimental constraints and predict a range of m_h values which are beyond the reach of CERN e^+e^- collider LEP experiments [22]. Interestingly, these large-tanβ solutions in non-minimal SUGRA models do admit positive values for $C_7^{\rm eff}(m_B)$ which are compatible in magnitude with the CLEO bounds. In a more general SUSY framework, the allowed parameter space for flavor-violating transitions is much larger. Thus, in the MIA approach [23], not only the sign of $C_7^{\rm eff}$ but also that of C_{10} may have either value. As different dilepton invariant mass regions in $B\to X_s l^+l^-$, the coefficients $C_7^{\rm eff}(m_B)$, $C_9^{\rm eff}(m_B)$ and C_{10} are weighted differently, a detailed knowledge of the invariant mass distribution and the FB asymmetry [28], together with the decay rate $B\to X_s\gamma$, is completely sufficient to determine these effective coefficients [17].[2] With obvious changes, these remarks apply to the exclusive decays $B\to(K,K^*)l^+l^-$ as well with the proviso that form factor dependence introduces an additional uncertainty, which we estimate in this paper. A relatively stable quantity is the

[1] In general, more operators are present in supersymmetric theories and we discuss their possible effects later in this paper.

[2] Note that $C_7^{\rm eff}$, C_9 and C_{10} are Wilson coefficients (numbers), but $C_9^{\rm eff}$ is a function of the dilepton invariant mass and encodes also the information from the long-distance contribution. We assume that new physics leaves the long-distance part largely intact.

TABLE I. Values of the SM Wilson coefficients used in the numerical calculations, corresponding to the central values of the parameters given in Table VI. Here, $C_7^{\rm eff}\equiv C_7-C_5/3-C_6$, and for C_9 we use the NDR scheme and $C^{(0)}\equiv 3C_1+C_2+3C_3+C_4+3C_5+C_6$.

C_1	C_2	C_3	C_4	C_5	C_6	$C_7^{\rm eff}$	C_9	C_{10}	$C^{(0)}$
-0.248	$+1.107$	$+0.011$	-0.026	$+0.007$	-0.031	-0.313	$+4.344$	-4.669	$+0.362$

value of the dilepton invariant mass for which the forward-backward FB asymmetry becomes zero in the SM. This has been discussed in the context of a number of phenomenological models for the form factors [44]. We argue here that using the results of the large-energy expansion technique (LEET) [58], the uncertainty in the zero of the FB asymmetry in the decays $B\to K^*l^+l^-$ due to the form factors can be shown to be minimal. This yields a strikingly simple relation between the coefficients $C_7{}^{\rm eff}$ and $C_9{}^{\rm eff}$ which we present in this paper.

This paper is organized as follows: In Sec. II, we introduce the effective Hamiltonian formalism for semileptonic rare B decays. Section III contains the definitions and derivations of the form factors in the decays $B\to(K,K^*)l^+l^-$ using the light cone QCD sum rule approach. In Sec. IV, we display the decay distributions for the invariant dilepton mass spectra for $B\to(K,K^*)l^+l^-$ and the FB asymmetry for $B\to K^*l^+l^-$. Section V contains our numerical results for the branching ratios and the FB asymmetry in the SM, including comparison with the available data. Comparative studies in a number of variants of the supersymmetric models are presented in Sec. VI. Section VII contains a brief summary and some concluding remarks.

II. EFFECTIVE HAMILTONIAN

At the quark level, the rare semileptonic decay $b\to sl^+l^-$ can be described in terms of the effective Hamiltonian obtained by integrating out the top quark and $W^\pm$ bosons:

$$\mathcal{H}_{\rm eff}=-4\frac{G_F}{\sqrt{2}}V_{ts}^*V_{tb}\sum_{i=1}^{10}C_i(\mu)\mathcal{O}_i(\mu). \tag{2.1}$$

In this paper, we use the Wilson-coefficients C_i calculated in the naive dimensional regularization (NDR) scheme [59].

The above Hamiltonian leads to the following free quark decay amplitude:

$$\begin{aligned}\mathcal{M}(b\to sl^+l^-)=\frac{G_F\alpha}{\sqrt{2}\,\pi}V_{ts}^*V_{tb}\Big\{&C_9{}^{\rm eff}[\bar{s}\gamma_\mu Lb][\bar{l}\gamma^\mu l]\\&+C_{10}[\bar{s}\gamma_\mu Lb][\bar{l}\gamma^\mu\gamma_5 l]\\&-2\hat{m}_bC_7{}^{\rm eff}\left[\bar{s}i\sigma_{\mu\nu}\frac{\hat{q}^\nu}{\hat{s}}Rb\right][\bar{l}\gamma^\mu l]\Big\}.\end{aligned} \tag{2.2}$$

Here, $L/R\equiv(1\mp\gamma_5)/2$, $s=q^2$, $q=p_++p_-$ where $p_\pm$ are the four-momenta of the leptons, respectively. We put $m_s/m_b=0$, but keep the leptons massive. The hat denotes normalization in terms of the B-meson mass, m_B, e.g. $\hat{s}=s/m_B^2$, $\hat{m}_b=m_b/m_B$. Here and in the remainder of this work we shall denote by $m_b\equiv m_b(\mu)$ the $\overline{\rm MS}$ mass evaluated at a scale μ and by $m_{b,pole}$ the pole mass of the b quark. To NLO in perturbation theory, they are related by

$$m_b(\mu)=m_{bpole}\left[1-\frac{4}{3}\frac{\alpha_s(\mu)}{\pi}\left\{1-\frac{3}{4}\ln\left(\frac{m_{bpole}^2}{\mu^2}\right)\right\}\right]. \tag{2.3}$$

Note that $\mathcal{M}(b\to sl^+l^-)$, although a free quark decay amplitude, contains certain long-distance effects from the matrix elements of four-quark operators, $\langle l^+l^-s|\mathcal{O}_i|b\rangle$, $1\leqslant i\leqslant 6$, which usually are absorbed into a redefinition of the short-distance Wilson coefficients. To be specific, we define, for exclusive decays,[3] the effective coefficient of the operator $\mathcal{O}_9=e^2/(16\pi^2)(\bar{s}\gamma_\mu Lb)(\bar{l}\gamma^\mu l)$ as

$$C_9{}^{\rm eff}(\hat{s})=C_9+Y(\hat{s}), \tag{2.4}$$

where $Y(\hat{s})$ stands for the above-mentioned matrix elements of the four-quark operators. A perturbative calculation yields [54,55]

$$\begin{aligned}Y_{\rm pert}(\hat{s})=&\,g(\hat{m}_c,\hat{s})(3C_1+C_2+3C_3+C_4+3C_5+C_6)\\&-\frac{1}{2}g(1,\hat{s})(4C_3+4C_4+3C_5+C_6)\\&-\frac{1}{2}g(0,\hat{s})(C_3+3C_4)+\frac{2}{9}(3C_3+C_4+3C_5+C_6).\end{aligned} \tag{2.5}$$

We work in leading logarithmic (LLog) approximation with the values of C_i given in Table I. Formulas can be seen in [54]. For the decays $B\to X_sl^+l^-$ [likewise, for $B\to(K,K^*)l^+l^-$], and with $\hat{s}$ far below the $c\bar{c}$ threshold, perturbation theory, augmented by power corrections, is expected to yield a reliable estimate. The power corrections in

[3]For *inclusive* decays one has in addition to take into account the $\mathcal{O}(\alpha_s)$ virtual and bremsstrahlung corrections to the matrix element $\langle l^+l^-s|\mathcal{O}_9|b\rangle$ as calculated in [60]. For *exclusive* decays, one can define an effective coefficient by including only the virtual corrections. We do not include any perturbative corrections to the partonic matrix elements. However, corresponding corrections are included in the nonperturbative matrix element over mesons.

TABLE II. Fudge factors in $B\to K^{(*)}J/\Psi,\Psi'\to K^{(*)}l^+l^-$ decays calculated using the LCSR form factors.

κ	J/Ψ	Ψ'
K	2.70	3.51
K^*	1.65	2.36

$1/m_c^2$ cannot be calculated near the threshold $s=4m_c^2$ and in the resonance regions, as the heavy quark expansion breaks down [27]. So, a complete profile of the FCNC semileptonic decays cannot at present be calculated from first principles. Several phenomenological prescriptions for incorporating the nonperturbative contributions to $Y(\hat{s})$ exist in the literature [28,29,31]. The resulting uncertainties on $C_9^{\rm eff}$ and various distributions in the inclusive decays have been worked out in [5,32,30] to which we refer for detailed discussions. In the present paper we use the two parametrizations due to Krüger and Sehgal [29] and Ali, Mannel and Morozumi [28], and interpret the difference in results for $C_9^{\rm eff}$ as an estimate of the theoretical uncertainty. Nonperturbative effects originate in particular from resonance corrections to the perturbative quark loops included in $Y_{\rm pert}(\hat{s})$. Light-quark loops are suppressed by small Wilson-coefficients, so it is essentially only the charm loop that matters. Reference [28] suggests to add the $c\bar{c}$ resonance contributions from $J/\Psi,\Psi',\ldots,\Psi^{(v)}$ to the perturbative result, with the former parametrized in the form of a phenomenological Breit-Wigner ansatz [36]. Y is then given by

$$Y_{\rm amm}(\hat{s})=Y_{\rm pert}(\hat{s})+\frac{3\pi}{\alpha^2}C^{(0)}\sum_{V_i=\psi(1s),\ldots,\psi(6s)}\kappa_i \times\frac{\Gamma(V_i\to l^+l^-)m_{V_i}}{m_{V_i}^2-\hat{s}m_B^2-im_{V_i}\Gamma_{V_i}} \tag{2.6}$$

with $C^{(0)}\equiv 3C_1+C_2+3C_3+C_4+3C_5+C_6$. The phenomenological factors κ_i correct for the factorization approximation which with $N_C=3$ (also called *naive factorization* [61]) gives a too small branching fraction for $B\to K^{(*)}V_i$. They can be fixed from

$$\mathcal{B}(B\to K^{(*)}V_i\to K^{(*)}l^+l^-)=\mathcal{B}(B\to K^{(*)}V_i)\mathcal{B}(V_i\to l^+l^-), \tag{2.7}$$

where the right-hand side is given by data [15]. While in the literature for *inclusive* $B\to X_s l^+l^-$ decays, one comes across a universal $\kappa_i(X_s)\equiv\kappa_1(X_s)=2.3$ [62], we have evaluated the individual factors for the lowest two $c\bar{c}$ resonances, shown in Table II. In our numerical analysis we use for the higher resonances $\Psi^{(ii)},\ldots,\Psi^{(v)}$ the average of J/Ψ and Ψ'. We have averaged over charged and neutral B mesons if data are available. Concentrating on J/Ψ only and assuming that the inclusive case X_s is saturated by K and K^*, we get $\kappa_1(X_s)=1.9$. Note that only the combination $|C^{(0)}\kappa_i|$ can be fixed from the $J/\psi,\psi'$ data. However, we treat the phase of the κ_i as fixed to the one in the factorization approach. This is substantiated by data in which the Bauer-Stech-Wirbel parameters a_1 and a_2 [63] are consistently determined, with a_1 coming out close to its perturbation theory value and the sign of a_2/a_1 is the one given by the factorization approach [64,61].

In the AMM approach, it is tacitly assumed that the extrapolation of the Breit-Wigner form away from the resonances could be used to estimate these power corrections reliably.

The KS approach [29], on the other hand, bypasses the perturbative-nonperturbative dichotomy by using the measured cross section $\sigma(e^+e^-\to$ hadrons) together with the assumption of quark-hadron duality for large $\hat{s}$ to reconstruct $Y(\hat{s})$ from its imaginary part by a dispersion relation. However, perturbative contributions in $\sigma(e^+e^-\to$ hadrons) and $B\to X_s l^+l^-$ are not identical. In particular, the perturbative part of $Y(\hat{s})$ has genuine hard contributions proportional to m_b^2, which can neither be ignored nor taken care of by the quark-duality argument. The issue in this approach remains as to how much of the genuine perturbative contribution in $B\to X_s l^+l^-$ arising from the $c\bar{c}$ continuum should be kept and there is at present no unique solution to this problem, as argued in [31] to which we refer for further discussion of this point. As stated earlier, we shall take the difference between the AAM-based and KS-based approaches for the long-distance contributions as a theoretical systematic error.

III. FORM FACTORS FROM QCD SUM RULES ON THE LIGHT CONE

Exclusive decays $B\to(K,K^*)l^+l^-$ are described in terms of matrix elements of the quark operators in Eq. (2.2) over meson states, which can be parametrized in terms of form factors.

Let us first define the form factors of the transition involving the pseudoscalar mesons $B\to K$. The non-vanishing matrix elements are $(q=p_B-p)$

$$\langle K(p)|\bar{s}\gamma_\mu b|B(p_B)\rangle=f_+(s)\left\{(p_B+p)_\mu-\frac{m_B^2-m_K^2}{s}q_\mu\right\}+\frac{m_B^2-m_K^2}{s}f_0(s)q_\mu, \tag{3.1}$$

and

$$\begin{aligned}\langle K(p)|\bar{s}\sigma_{\mu\nu}q^\nu(1+\gamma_5)b|B(p_B)\rangle&\equiv\langle K(p)|\bar{s}\sigma_{\mu\nu}q^\nu b|B(p_B)\rangle\\&=i\{(p_B+p)_\mu s-q_\mu(m_B^2-m_K^2)\}\frac{f_T(s)}{m_B+m_K}.\end{aligned} \tag{3.2}$$

For the vector meson K^* with polarization vector ϵ_μ, we can define the semileptonic form factors of the $V-A$ current by

TABLE III. Central values of parameters for the parametrization (3.7) of the $B\to K$ and $B\to K^*$ form factors. Renormalization scale for the penguin form factors f_T and T_i is $\mu=m_b$. c_3 can be neglected for $B\to K^*$ form factors.

	f_+	f_0	f_T	A_1	A_2	A_0	V	T_1	T_2	T_3
$F(0)$	0.319	0.319	0.355	0.337	0.282	0.471	0.457	0.379	0.379	0.260
c_1	1.465	0.633	1.478	0.602	1.172	1.505	1.482	1.519	0.517	1.129
c_2	0.372	−0.095	0.373	0.258	0.567	0.710	1.015	1.030	0.426	1.128
c_3	0.782	0.591	0.700	0	0	0	0	0	0	0

$$\begin{aligned}\langle K^*(p)|(V-A)_\mu|B(p_B)\rangle=&-i\epsilon_\mu^*(m_B+m_{K*})A_1(s)\\&+i(p_B+p)_\mu(\epsilon^*p_B)\frac{A_2(s)}{m_B+m_{K*}}\\&+iq_\mu(\epsilon^*p_B)\frac{2m_{K*}}{s}\\&\times(A_3(s)-A_0(s))\\&+\epsilon_{\mu\nu\rho\sigma}\epsilon^{*\nu}p_B^\rho p^\sigma\frac{2V(s)}{m_B+m_{K*}}.\end{aligned}\tag{3.3}$$

Note the exact relations

$$\begin{aligned}A_3(s)&=\frac{m_B+m_{K*}}{2m_{K*}}A_1(s)-\frac{m_B-m_{K*}}{2m_{K*}}A_2(s),\\A_0(0)&=A_3(0),\\\langle K^*|\partial_\mu A^\mu|B\rangle&=2m_{K*}(\epsilon^*p_B)A_0(s).\end{aligned}\tag{3.4}$$

The second relation in Eq. (3.4) ensures that there is no kinematical singularity in the matrix element at $s=0$. The decay $B\to K^*l^+l^-$ is described by the above semileptonic form factors and the following penguin form factors:

$$\begin{aligned}&\langle K^*|\bar{s}\sigma_{\mu\nu}q^\nu(1+\gamma_5)b|B(p_B)\rangle\\&\quad=i\epsilon_{\mu\nu\rho\sigma}\epsilon^{*\nu}p_B^\rho p^\sigma 2T_1(s)+T_2(s)\\&\qquad\times\{\epsilon_\mu^*(m_B^2-m_{K^*}^2)-(\epsilon^*p_B)(p_B+p)_\mu\}\\&\qquad+T_3(s)(\epsilon^*p_B)\left\{q_\mu-\frac{s}{m_B^2-m_{K^*}^2}(p_B+p)_\mu\right\}\end{aligned}\tag{3.5}$$

with

$$T_1(0)=T_2(0).\tag{3.6}$$

All signs are defined in such a way as to render the form factors positive. The physical range in s extends from $s_{\min}=0$ to $s_{\max}=(m_B-m_{K,K*})^2$.

Lacking a complete solution of non-perturbative QCD, one has to rely on certain approximate methods to calculate the above form factors. In this paper, we choose to calculate them by the QCD sum rules on the light cone (LCSRs). The method of LCSRs was first suggested for the study of weak baryon decays in [45] and later extended to heavy meson decays in [46]. It is a nonperturbative approach which combines ideas of QCD sum rules [65] with the twist expansion characteristic for hard exclusive processes in QCD [66] and makes explicit use of the large energy of the final state meson at small values of the momentum transfer to leptons s. In this respect, the LCSR approach is complementary to lattice calculations [67], which are mainly restricted to form factors at small recoil (large values of s) and at present require the scaling behavior found in the context of the LCSRs to extrapolate to smaller values of s [68]. Of course, the LCSRs lack the rigor of the lattice approach. Nevertheless, they provide a powerful nonperturbative model which is explicitly consistent with perturbative QCD and the heavy quark limit.

Early studies of exclusive B decays in the LCSR approach were restricted to contributions of leading twist and did not take into account radiative corrections. These corrections, included in the estimates presented here, turn out to shift the form factors by $\sim 10\%$.

In previous works [69,52,49], the resulting form factors have been parametrized by a modified single pole formula,

$$F(\hat{s})=\frac{F(0)}{1-a_F\hat{s}+b_F\hat{s}^2},$$

obtained from a fit to the LCSR result in the region $\hat{s}<0.54$. The extrapolation of this parametrization to maximum $\hat{s}$ is prone to spurious singularities below the physical cut starting at $s=m_{B_s^*}^2$. In the present work we thus choose a different parametrization which avoids this problem:

$$F(\hat{s})=F(0)\exp(c_1\hat{s}+c_2\hat{s}^2+c_3\hat{s}^3).\tag{3.7}$$

The term in $\hat{s}^3$ turns out to be important in $B\to K$ transitions, where $\hat{s}$ can be as large as 0.82, but can be neglected for $B\to K^*$ with $\hat{s}<0.69$. The parametrization formula works within 1% accuracy for $s<15$ GeV^2. For an estimate of the theoretical uncertainty of these form factors, we have varied the input parameters of the LCSRs, i.e. the b quark mass, the Gegenbauer moments of the K and K^* distribution amplitudes and the LCSR-specific Borel-parameters M^2 and continuum threshold s_0 within their respective allowed ranges specified in [52,49] and obtain the three sets of form factors given in Tables III–V, which represent, for each $\hat{s}$, the cen-

TABLE IV. Parameters for the maximum allowed form factors.

	f_+	f_0	f_T	A_1	A_2	A_0	V	T_1	T_2	T_3
$F(0)$	0.371	0.371	0.423	0.385	0.320	0.698	0.548	0.437	0.437	0.295
c_1	1.412	0.579	1.413	0.557	1.083	1.945	1.462	1.498	0.495	1.044
c_2	0.261	−0.240	0.247	0.068	0.393	0.314	0.953	0.976	0.402	1.378
c_3	0.822	0.774	0.742	0	0	0	0	0	0	0

tral value, maximum and minimum allowed form factor, respectively. We plot the form factors in Figs. 1 and 2.

Our value of $T_1(0)$ is consistent with the CLEO measurement of $\mathcal{B}(B\to K^*\gamma)_{exp}=(4.2\pm 0.8\pm 0.6)\times 10^{-5}$ [70]. From the formula for the decay rate,

$$\Gamma(B\to K^*\gamma)=\frac{G_F^2\alpha|V_{ts}^*V_{tb}|^2}{32\pi^4}m_b^2m_B^3 \times(1-m_{K*}^2/m_B^2)^3|C_7^{\rm eff}|^2|T_1(0)|^2, \tag{3.8}$$

the central values of the parameters given in Table VI, $T_1(0)=0.379$ and with $\tau_B=1.61$ ps we find $\mathcal{B}(B\to K^*\gamma)_{th}=4.4\times 10^{-5}$.

IV. DECAY DISTRIBUTIONS

In this section we define various decay distributions whose phenomenological analysis will be performed in the next section.

Equation (2.2) can be written as

$$\mathcal{M}=\frac{G_F\alpha}{2\sqrt{2}\pi}V_{ts}^*V_{tb}m_B[\mathcal{T}_\mu^1(\bar{l}\gamma^\mu)+\mathcal{T}_\mu^2(\bar{l}\gamma^\mu\gamma_5 l)], \tag{4.1}$$

where for $B\to Kl^+l^-$,

$$\mathcal{T}_\mu^1=A'(\hat{s})\hat{p}_{h\mu}+B'(\hat{s})\hat{q}_\mu, \tag{4.2}$$

$$\mathcal{T}_\mu^2=C'(\hat{s})\hat{p}_{h\mu}+D'(\hat{s})\hat{q}_\mu, \tag{4.3}$$

and for $B\to K^*l^+l^-$,

$$\mathcal{T}_\mu^1=A(\hat{s})\epsilon_{\mu\rho\alpha\beta}\epsilon^{*\rho}\hat{p}_B^\alpha\hat{p}_{K*}^\beta-iB(\hat{s})\epsilon^*{}_\mu+iC(\hat{s})(\epsilon^*\cdot\hat{p}_B)\hat{p}_{h\mu} +iD(\hat{s})(\epsilon^*\cdot\hat{p}_B)\hat{q}_\mu, \tag{4.4}$$

$$\mathcal{T}_\mu^2=E(\hat{s})\epsilon_{\mu\rho\alpha\beta}\epsilon^{*\rho}\hat{p}_B^\alpha\hat{p}_{K*}^\beta-iF(\hat{s})\epsilon^*{}_\mu+iG(\hat{s})(\epsilon^*\cdot\hat{p}_B)\hat{p}_{h\mu} +iH(\hat{s})(\epsilon^*\cdot\hat{p}_B)\hat{q}_\mu, \tag{4.5}$$

with $p\equiv p_B+p_{K,K^*}$. Note that, using the equation of motion for lepton fields, the terms in $\hat{q}_\mu$ in $\mathcal{T}_\mu^1$ vanish and those in $\mathcal{T}_\mu^2$ become suppressed by one power of the lepton mass. This effectively eliminates the photon pole in B' for $B\to K$.

The auxiliary functions above are defined as

$$A'(\hat{s})=C_9{}^{\rm eff}(\hat{s})f_+(\hat{s})+\frac{2\hat{m}_b}{1+\hat{m}_K}C_7{}^{\rm eff}f_T(\hat{s}), \tag{4.6}$$

$$B'(\hat{s})=C_9{}^{\rm eff}(\hat{s})f_-(\hat{s})-\frac{2\hat{m}_b}{\hat{s}}(1-\hat{m}_K)C_7{}^{\rm eff}f_T(\hat{s}), \tag{4.7}$$

$$C'(\hat{s})=C_{10}f_+(\hat{s}), \tag{4.8}$$

$$D'(\hat{s})=C_{10}f_-(\hat{s}), \tag{4.9}$$

$$A(\hat{s})=\frac{2}{1+\hat{m}_{K*}}C_9{}^{\rm eff}(\hat{s})V(\hat{s})+\frac{4\hat{m}_b}{\hat{s}}C_7{}^{\rm eff}T_1(\hat{s}), \tag{4.10}$$

$$B(\hat{s})=(1+\hat{m}_{K*})\left[C_9{}^{\rm eff}(\hat{s})A_1(\hat{s}) +\frac{2\hat{m}_b}{\hat{s}}(1-\hat{m}_{K*})C_7{}^{\rm eff}T_2(\hat{s})\right], \tag{4.11}$$

$$C(\hat{s})=\frac{1}{1-\hat{m}_{K*}^2}\left[(1-\hat{m}_{K*})C_9{}^{\rm eff}(\hat{s})A_2(\hat{s}) +2\hat{m}_bC_7{}^{\rm eff}\left(T_3(\hat{s})+\frac{1-\hat{m}_{K*}^2}{\hat{s}}T_2(\hat{s})\right)\right], \tag{4.12}$$

TABLE V. Parameters for the minimum allowed form factors.

	f_+	f_0	f_T	A_1	A_2	A_0	V	T_1	T_2	T_3
$F(0)$	0.278	0.278	0.300	0.294	0.246	0.412	0.399	0.334	0.334	0.234
c_1	1.568	0.740	1.600	0.656	1.237	1.543	1.537	1.575	0.562	1.230
c_2	0.470	0.080	0.501	0.456	0.822	0.954	1.123	1.140	0.481	1.089
c_3	0.885	0.425	0.796	0	0	0	0	0	0	0

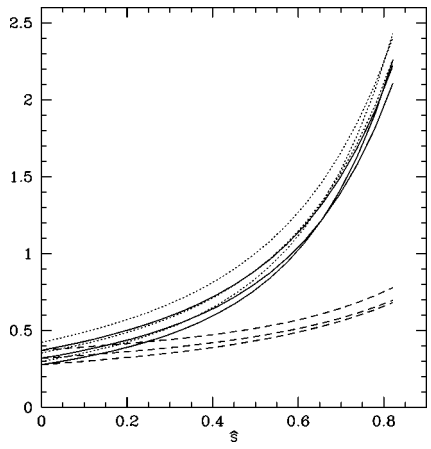

FIG. 1. LCSR form factors with theoretical uncertainties for the $B\to K$ transition as a function of $\hat{s}$. Solid, dotted and dashed curves correspond to f_+, f_T, f_0, respectively. Renormalization scale for f_T is $\mu=m_b$.

$$D(\hat{s})=\frac{1}{\hat{s}}[C_9{}^{\rm eff}(\hat{s})((1+\hat{m}_{K^*})A_1(\hat{s})-(1-\hat{m}_{K^*})A_2(\hat{s}) -2\hat{m}_{K^*}A_0(\hat{s}))-2\hat{m}_b C_7{}^{\rm eff}T_3(\hat{s})], \tag{4.13}$$

$$E(\hat{s})=\frac{2}{1+\hat{m}_{K^*}}C_{10}V(\hat{s}), \tag{4.14}$$

$$F(\hat{s})=(1+\hat{m}_{K^*})C_{10}A_1(\hat{s}), \tag{4.15}$$

$$G(\hat{s})=\frac{1}{1+\hat{m}_{K^*}}C_{10}A_2(\hat{s}), \tag{4.16}$$

$$H(\hat{s})=\frac{1}{\hat{s}}C_{10}[(1+\hat{m}_{K^*})A_1(\hat{s})-(1-\hat{m}_{K^*})A_2(\hat{s}) -2\hat{m}_{K^*}A_0(\hat{s})]. \tag{4.17}$$

Note that the inclusion of the full s-quark mass dependence into the above formulas can be done by substituting $m_b \to m_b+m_s$ into all terms proportional to $C_7{}^{\rm eff}T_1$ and $C_7{}^{\rm eff}f_T$ and $m_b\to m_b-m_s$ in $C_7{}^{\rm eff}T_{2,3}$, since $O_7\sim\bar{s}\sigma_{\mu\nu}[(m_b+m_s)+(m_b-m_s)\gamma_5]q^\nu b$.

TABLE VI. Default values of the input parameters and the ±1 σ errors on the sensitive parameters used in our numerical calculations.

m_W	80.41 GeV
m_Z	91.1867 GeV
$\sin^2\theta_W$	0.2233
m_c	1.4 GeV
m_{bpole}	4.8 ± 0.2 GeV
m_t	173.8 ± 5.0 GeV
μ	$m_{b,pole}{}^{+m_{b,pole}}_{-m_{b,pole}/2}$
$\Lambda^{(5)}_{QCD}$	$0.220^{+0.078}_{-0.063}$ GeV
α^{-1}	129
$\alpha_s(m_Z)$	0.119 ± 0.0058
$\lvert V_{ts}^*V_{tb}\rvert$	0.0385
$\lvert V_{ts}^*V_{tb}\rvert/\lvert V_{cb}\rvert$	1

We choose the kinematic variables $(\hat{s},\hat{u})$ to be

$$\hat{s}=\hat{q}^2=(p_+ + p_-)^2, \tag{4.18}$$

$$\hat{u}=(\hat{p}_B-p_-)^2-(\hat{p}_B-p_+)^2 \tag{4.19}$$

which are bounded as

$$(2\hat{m}_l)^2\leqslant\hat{s}\leqslant(1-\hat{m}_{K,K^*})^2, \tag{4.20}$$

$$-\hat{u}(\hat{s})\leqslant\hat{u}\leqslant\hat{u}(\hat{s}), \tag{4.21}$$

with $\hat{m}_l=m_l/m_B$ and

$$\hat{u}(\hat{s})=\sqrt{\lambda\left(1-4\frac{\hat{m}_l^2}{\hat{s}}\right)}, \tag{4.22}$$

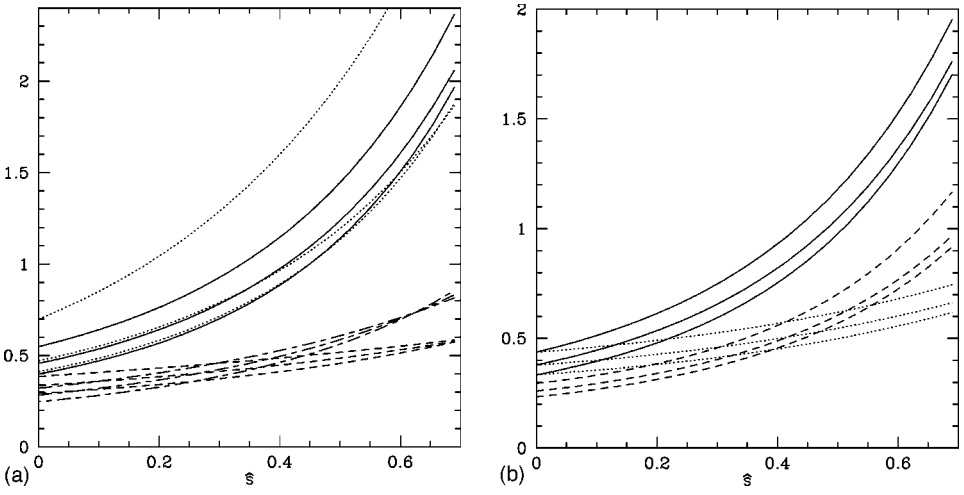

FIG. 2. LCSR form factors with theoretical uncertainties for the $B\to K^*$ transition as a function of $\hat{s}$. In (a), the solid, dotted, dashed and short long dashed curves correspond to V, A_0, A_1, A_2 and in (b) the solid, dotted and dashed curves correspond to T_1, T_2, T_3, respectively. Renormalization scale for T_i is $\mu=m_b$.

$$\lambda \equiv \lambda(1,\hat{m}_{K,K*}^2,\hat{s}) = 1+\hat{m}_{K,K*}^4+\hat{s}^2-2\hat{s}-2\hat{m}_{K,K*}^2(1+\hat{s}). \tag{4.23}$$

Note that the variable $\hat{u}$ corresponds to θ, the angle between the momentum of the B meson and the positively charged lepton l^+ in the dilepton c.m. system (c.m.s.) frame, through the relation $\hat{u}=-\hat{u}(\hat{s})\cos\theta$ [28]. Keeping the lepton mass, we find the double differential decay widths Γ^K and Γ^{K^*} for the decays $B\to Kl^+l^-$ and $B\to K^*l^+l^-$, respectively, as

$$\frac{d^2\Gamma^K}{d\hat{s}d\hat{u}}=\frac{G_F^2\alpha^2 m_B^5}{2^{11}\pi^5}|V_{ts}^*V_{tb}|^2\{(|A'|^2+|C'|^2)(\lambda-\hat{u}^2)+|C'|^2 4\hat{m}_l^2(2+2\hat{m}_K^2-\hat{s})+\mathrm{Re}(C'D'^*)8\hat{m}_l^2(1-\hat{m}_K^2)+|D'|^2 4\hat{m}_l^2\hat{s}\}, \tag{4.24}$$

$$\begin{aligned}\frac{d^2\Gamma^{K^*}}{d\hat{s}d\hat{u}}=&\frac{G_F^2\alpha^2 m_B^5}{2^{11}\pi^5}|V_{ts}^*V_{tb}|^2\Bigg\{\frac{|A|^2}{4}(\hat{s}(\lambda+\hat{u}^2)+4\hat{m}_l^2\lambda)+\frac{|E|^2}{4}(\hat{s}(\lambda+\hat{u}^2)-4\hat{m}_l^2\lambda)+\frac{1}{4\hat{m}_{K*}^2}[|B|^2(\lambda-\hat{u}^2+8\hat{m}_{K*}^2(\hat{s}+2\hat{m}_l^2))\\&+|F|^2(\lambda-\hat{u}^2+8\hat{m}_{K*}^2(\hat{s}-4\hat{m}_l^2))]-2\hat{s}\hat{u}[\mathrm{Re}(BE^*)+\mathrm{Re}(AF^*)]+\frac{\lambda}{4\hat{m}_{K*}^2}[|C|^2(\lambda-\hat{u}^2)\\&+|G|^2(\lambda-\hat{u}^2+4\hat{m}_l^2(2+2\hat{m}_{K*}^2-\hat{s}))]-\frac{1}{2\hat{m}_{K*}^2}[\mathrm{Re}(BC^*)(1-\hat{m}_{K*}^2-\hat{s})(\lambda-\hat{u}^2)+\mathrm{Re}(FG^*)\\&\times((1-\hat{m}_{K*}^2-\hat{s})(\lambda-\hat{u}^2)+4\hat{m}_l^2\lambda)]-2\frac{\hat{m}_l^2}{\hat{m}_{K*}^2}\lambda[\mathrm{Re}(FH^*)-\mathrm{Re}(GH^*)(1-\hat{m}_{K*}^2)]+|H|^2\frac{\hat{m}_l^2}{\hat{m}_{K*}^2}\hat{s}\lambda\Bigg\}.\end{aligned} \tag{4.25}$$

A. Dilepton mass spectrum

We now give formulas for the dilepton invariant mass spectra. Integrating over $\hat{u}$ in the kinematical region given in Eq. (4.21) we find

$$\begin{aligned}\frac{d\Gamma^K}{d\hat{s}}=&\frac{G_F^2\alpha^2 m_B^5}{2^{10}\pi^5}|V_{ts}^*V_{tb}|^2\hat{u}(\hat{s})\Bigg\{(|A'|^2+|C'|^2)\left(\lambda-\frac{\hat{u}(\hat{s})^2}{3}\right)+|C'|^2 4\hat{m}_l^2(2+2\hat{m}_K^2-\hat{s})\\&+\mathrm{Re}(C'D'^*)8\hat{m}_l^2(1-\hat{m}_K^2)+|D'|^2 4\hat{m}_l^2\hat{s}\Bigg\},\end{aligned} \tag{4.26}$$

$$\begin{aligned}\frac{d\Gamma^{K^*}}{d\hat{s}}=&\frac{G_F^2\alpha^2 m_B^5}{2^{10}\pi^5}|V_{ts}^*V_{tb}|^2\hat{u}(\hat{s})\Bigg\{\frac{|A|^2}{3}\hat{s}\lambda\left(1+2\frac{\hat{m}_l^2}{\hat{s}}\right)+|E|^2\hat{s}\frac{\hat{u}(\hat{s})^2}{3}+\frac{1}{4\hat{m}_{K*}^2}\\&\times\left[|B|^2\left(\lambda-\frac{\hat{u}(\hat{s})^2}{3}+8\hat{m}_{K*}^2(\hat{s}+2\hat{m}_l^2)\right)+|F|^2\left(\lambda-\frac{\hat{u}(\hat{s})^2}{3}+8\hat{m}_{K*}^2(\hat{s}-4\hat{m}_l^2)\right)\right]\\&+\frac{\lambda}{4\hat{m}_{K*}^2}\left[|C|^2\left(\lambda-\frac{\hat{u}(\hat{s})^2}{3}\right)+|G|^2\left(\lambda-\frac{\hat{u}(\hat{s})^2}{3}+4\hat{m}_l^2(2+2\hat{m}_{K*}^2-\hat{s})\right)\right]\\&-\frac{1}{2\hat{m}_{K*}^2}\left[\mathrm{Re}(BC^*)\left(\lambda-\frac{\hat{u}(\hat{s})^2}{3}\right)(1-\hat{m}_{K*}^2-\hat{s})+\mathrm{Re}(FG^*)\left(\left(\lambda-\frac{\hat{u}(\hat{s})^2}{3}\right)(1-\hat{m}_{K*}^2-\hat{s})+4\hat{m}_l^2\lambda\right)\right]\\&-2\frac{\hat{m}_l^2}{\hat{m}_{K*}^2}\lambda[\mathrm{Re}(FH^*)-\mathrm{Re}(GH^*)(1-\hat{m}_{K*}^2)]+\frac{\hat{m}_l^2}{\hat{m}_{K*}^2}\hat{s}\lambda|H|^2\Bigg\}.\end{aligned} \tag{4.27}$$

Both distributions agree with the ones obtained in [42]. In the limit $m_l\to 0$ the form factors f_0 (or f_-) and A_0 do not contribute. Furthermore, since $|C_7^{\mathrm{eff}}|\ll|C_9^{\mathrm{eff}}|,|C_{10}|$, the influence of f_T,T_3 on the distributions is subdominant. That means

that roughly $d\Gamma^K/d\hat{s}\sim|f_+|^2$ for $l=e,\mu$ in the low $\hat{s}$ region below the J/Ψ, with a $\sim-12\%$ effect coming from $C_7^{\rm eff}f_T$ terms. For $B\to K^*$, the $b\to s\gamma$ transition is more important: for $s<1$ GeV^2 the photon pole is the dominant contribution, and it still contributes $\sim-30\%$ around $s\approx 3$ GeV^2.

B. Forward-backward asymmetry

The differential forward-backward asymmetry (FBA) is defined as [28]

$$\frac{d\mathcal{A}_{\rm FB}}{d\hat{s}}=-\int_0^{\hat{u}(\hat{s})}d\hat{u}\frac{d^2\Gamma}{d\hat{u}\,d\hat{s}}+\int_{-\hat{u}(\hat{s})}^{0}d\hat{u}\frac{d^2\Gamma}{d\hat{u}\,d\hat{s}}. \tag{4.28}$$

The FBA vanishes in $B\to Kl^+l^-$ decays as can be seen from Eq. (4.24), since there is no term containing $\hat{u}$ with an odd power. For $B\to K^*l^+l^-$ decays it reads as follows:

$$\begin{aligned}\frac{d\mathcal{A}_{\rm FB}}{d\hat{s}}&=\frac{G_F^2\alpha^2m_B^5}{2^{10}\pi^5}|V_{ts}^*V_{tb}|^2\hat{s}\hat{u}(\hat{s})^2[{\rm Re}(BE^*)+{\rm Re}(AF^*)]\\&=\frac{G_F^2\alpha^2m_B^5}{2^8\pi^5}|V_{ts}^*V_{tb}|^2\hat{s}\hat{u}(\hat{s})^2C_{10}\left[{\rm Re}(C_9^{\rm eff})VA_1+\frac{\hat{m}_b}{\hat{s}}C_7^{\rm eff}(VT_2(1-\hat{m}_{K^*})+A_1T_1(1+\hat{m}_{K^*}))\right].\end{aligned} \tag{4.29}$$

The position of the zero $\hat{s}_0$ is given by

$${\rm Re}(C_9^{\rm eff}(\hat{s}_0))=-\frac{\hat{m}_b}{\hat{s}_0}C_7^{\rm eff}\left\{\frac{T_2(\hat{s}_0)}{A_1(\hat{s}_0)}(1-\hat{m}_{K^*})+\frac{T_1(\hat{s}_0)}{V(\hat{s}_0)}(1+\hat{m}_{K^*})\right\}, \tag{4.30}$$

which depends on the value of m_b, the ratio of the effective coefficients $C_7^{\rm eff}/{\rm Re}(C_9^{\rm eff}(\hat{s}_0))$, and the ratio of the form factors shown above. It is interesting to observe that in the Large Energy Effective Theory (LEET) [58], both ratios of the form factors appearing in Eq. (4.30) have essentially no hadronic uncertainty, i.e., all dependence on the intrinsically nonperturbative quantities cancels, and one has simply

$$\begin{aligned}\frac{T_2}{A_1}&=\frac{1+\hat{m}_{K^*}}{1+\hat{m}_{K^*}^2-\hat{s}}\left(1-\frac{\hat{s}}{1-\hat{m}_{K^*}^2}\right),\\\frac{T_1}{V}&=\frac{1}{1+\hat{m}_{K^*}}.\end{aligned} \tag{4.31}$$

With these relations, one has a particularly simple form for the equation determining $\hat{s}_0$, namely

$${\rm Re}(C_9^{\rm eff}(\hat{s}_0))=-2\frac{\hat{m}_b}{\hat{s}_0}C_7^{\rm eff}\frac{1-\hat{s}_0}{1+m_{K^*}^2-\hat{s}_0}. \tag{4.32}$$

Thus, the precision on the zero point of the FB asymmetry in $B\to K^*l^+l^-$ is determined essentially by the precision of the ratio of the effective coefficients and m_b, making it at par with the corresponding quantity in the inclusive decays $B\to X_sl^+l^-$, for which the zero point is given by the solution of the equation ${\rm Re}(C_9^{\rm eff}(\hat{s}_0))=-(2/\hat{s}_0)C_7^{\rm eff}$. We find the insensitivity of $\hat{s}_0$ to the decay form factors in $B\to K^*l^+l^-$ a remarkable result, which has also been discussed in [44]. However, the LEET-based result in Eq. (4.31) stands theoretically on more rigorous grounds than the arguments based on scanning a number of form factor models. With the coefficients given in Table I and $m_b=4.4$ GeV, we find $\hat{s}_0=0.10$ (i.e. $s_0=2.9$ GeV^2) in the SM. From Eq. (4.30) it follows that there is no zero below the $c\bar{c}$ resonances if both C_9 and $C_7^{\rm eff}$ have the same sign as predicted in some beyond-the-SM models.

From the experimental point of view the normalized FB asymmetry is more useful, defined as

$$\frac{d\bar{\mathcal{A}}_{\rm FB}}{d\hat{s}}=\frac{d\mathcal{A}_{\rm FB}}{d\hat{s}}\Big/\frac{d\Gamma}{d\hat{s}} \tag{4.33}$$

which is equivalent to the energy asymmetry [18,25]. A slightly different definition is

$$\frac{d\mathcal{A}'_{\rm FB}}{d\hat{s}}=\frac{d\mathcal{A}_{\rm FB}}{d\hat{s}}\Big/\Gamma \tag{4.34}$$

whose integral gives the *global* energy asymmetry $\mathcal{A}'_{FB}=\mathcal{A}_{FB}/\Gamma$.

We summarize the characteristics of our observables:

$(d\mathcal{B}/ds)(B\to Kl^+l^-)$ and $(d\mathcal{B}/ds)(B\to K^*l^+l^-)$ get maximal for maximal $|C_7^{\rm eff}|,|C_9|,|C_{10}|$ and ${\rm sign}(C_7^{\rm eff}{\rm Re}(C_9^{\rm eff}))=+1$.

$(d\bar{\mathcal{A}}_{FB}/ds)(B\to K^* l^+ l^-)$ is proportional to C_{10} and has a characteristic zero (barring the trivial solution $C_{10}=0$, which we do not entertain here) if Eq. (4.30) is satisfied, which requires

$$\text{sign}(C_7^{\text{eff}}\text{Re}(C_9^{\text{eff}}))=-1. \tag{4.35}$$

The condition in Eq. (4.35) provides a discrimination between the SM and models having new physics. For example, this condition is satisfied in the SM and the SUGRA models with low-tan β, in which case the actual position of $\hat{s}_0$ would provide the further discriminant. However, it turns out that the allowed parameter space of the SUGRA models with large-tan β yield $\text{sign}(C_7^{\text{eff}}\text{Re}(C_9^{\text{eff}}))=+1$ [22], leading to the result that the FB asymmetry in these models is parametrically different. In particular, in all such cases, there is no zero of the FB asymmetry.

V. BRANCHING RATIOS AND FB ASYMMETRY IN SM

The input parameters that we use in our numerical analysis are given in Table VI. The parameters which are either well known or have a small influence on the decay rates have been fixed to their central values, but we vary four of the listed parameters, m_t, μ, $m_{b,pole}$ and $\alpha_s(m_Z)$, in the indicated range. Furthermore, in the evaluation of the various distributions we use for $\hat{m}_b$ the MSbar mass evaluated at the scale $\mu=m_{b,pole}$, see Eq. (2.3). In the SM we obtain the following non-resonant branching ratios, denoted by $\mathcal{B}_{nr}$ ($l=e,\mu$):

$$\mathcal{B}_{nr}(B\to Kl^+l^-)=5.7\times10^{-7},$$

$$\Delta\mathcal{B}_{nr}=(^{+27}_{-15},\pm6,^{+7}_{-6},\pm1,\pm2)\%, \tag{5.1}$$

$$\mathcal{B}_{nr}(B\to K\tau^+\tau^-)=1.3\times10^{-7},$$

$$\Delta\mathcal{B}_{nr}=(^{+22}_{-6},\pm7,^{+4}_{-3},^{+0.4}_{-0.2},\pm1)\%, \tag{5.2}$$

$$\mathcal{B}_{nr}(B\to K^*e^+e^-)=2.3\times10^{-6},$$

$$\Delta\mathcal{B}_{nr}=(^{+29}_{-17},^{+2}_{-9},+12,^{+4}_{-1},\pm3)\%, \tag{5.3}$$

$$\mathcal{B}_{nr}(B\to K^*\mu^+\mu^-)=1.9\times10^{-6},$$

$$\Delta\mathcal{B}_{nr}=(^{+26}_{-17},\pm6,^{+6}_{-4},^{-0.7}_{+0.4},\pm2)\%, \tag{5.4}$$

$$\mathcal{B}_{nr}(B\to K^*\tau^+\tau^-)=1.9\times10^{-7},$$

$$\Delta\mathcal{B}_{nr}=(^{+4}_{-8},\pm4,^{+13}_{-11},^{+0.6}_{-0.3},\pm3)\%. \tag{5.5}$$

The first error in the $\Delta\mathcal{B}_{nr}$ consists of hadronic uncertainties from the form factors. The other four errors given in the parentheses are due to the variations of m_t, μ, $m_{b,pole}$ and $\alpha_s(m_Z)$, in order of appearance. In addition, there is an error of $\pm2.5\%$ from the lifetimes τ_B [15]. The scale dependence of the branching ratio $\mathcal{B}_{nr}(B\to K^*e^+e^-)$ gives $+12\%$ and $+1.4\%$, as μ is varied from $\mu=m_{b,pole}$ to $\mu=m_{b,pole}/2$ and $\mu=2m_{b,pole}$, respectively, and we have taken the larger of

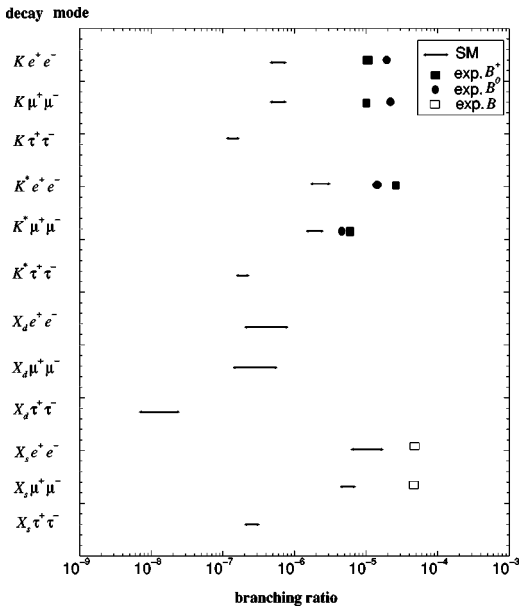

FIG. 3. Theoretical expectations for the exclusive decay branching ratios $\mathcal{B}(B\to K^*l^+l^-)$, $\mathcal{B}(B\to Kl^+l^-)$, $l^\pm=e^\pm,\mu^\pm,\tau^\pm$, calculated in the LCSR method in the SM. For the sake of completeness, we also give the branching ratios for the inclusive decays $B\to X_s l^+l^-$ and $B\to X_d l^+l^-$ in the SM, including the CKM dependence of the latter. Experimental upper limits (at 90% C.L.) are also shown: solid squares are from the charged B^+ decays (and charge conjugate), circles from the decays of B^0 (and charge conjugate), and the empty squares are from the inclusive decays, averaged over the charged and neutral B decays. All experimental limits are from the CLEO [35,33] and CDF [34] Collaborations.

the two errors in this case to estimate the scale dependence of this branching ratio. The largest parametric errors are from the uncertainties of the scale μ and the top quark mass, m_t. The large scale dependence of the branching ratios reflects essentially that of the effective coefficients. To remedy this, one has to calculate the virtual corrections to the matrix elements of the partonic decays $b\to sl^+l^-$ to obtain perturbatively improved effective coefficients which are both scale and scheme independent [71]. The exclusive decay form factors, obtained in the LCSR method including the radiative corrections, depend also on m_b, α_s and the renormalization scale μ. However, the various dependencies of the form factors are inadequate to compensate for the corresponding dependencies in the effective coefficients being used. We present in Fig. 3 the exclusive branching ratios calculated in the LCSR approach, obtained by adding the stated errors in quadrature. We also give, for the sake of completeness, the branching ratios for the inclusive decays $B\to(X_s,X_d)l^+l^-$. In calculating the theoretical dispersion on $B\to X_d l^+l^-$, we have varied the CKM parameters in the allowed range obtained from the CKM unitarity fits [12]. We have also listed the present experimental bounds on the exclusive decays $B\to(K,K^*)e^+e^-$ and $B\to(K,K^*)\mu^+\mu^-$, obtained by the CDF [34] and CLEO [35] Collaborations. Experimental upper limits on the inclusive decays $B\to X_s e^+e^-$ and $B\to X_s\mu^+\mu^-$ are from the CLEO Collaboration [33]. All experimental limits are 90% C.L., and for the sake of this fig-

ure we have averaged the branching ratios for the charged and neutral B-meson decays, as the differences in their branching ratios are expected to be minimal theoretically.

Figure 3 shows that the exclusive decays $B\to K^*\mu^+\mu^-$ and $B\to K^*e^+e^-$ provide at present the most stringent bounds on the effective coefficients. While none of the experimental bounds has reached the SM sensitivity, they do provide interesting upper limits on the parameter space of models with physics beyond the SM. We will discuss this point in detail below in the context of the SUSY models we are studying in this paper. We have also estimated the present theoretical precision on the quantity s_0 (zero of the FB asymmetry) in the decay $B\to K^*l^+l^-$ for $l^\pm=e^\pm$ and $l^\pm=\mu^\pm$. Note, that due to the kinematics, there is no zero for the FB asymmetry for the case $B\to K^*\tau^+\tau^-$. Theoretical uncertainties from the form factors and the four parameters discussed above, m_t, μ, $m_{b,pole}$ and $\alpha_s(m_Z)$, on the s_0 are estimated as $\pm 1\%, \pm 0.3\%, +14\%/-7\%, \pm 6\%, \pm 4\%$, respectively. As discussed above, the form factor-dependent uncertainty for this quantity is minimal, and the main sources of errors are μ and $m_{b,pole}$. The reason of the marked scale dependence is again the lack of compensating perturbative corrections, in the absence of which the scale dependence of the Wilson coefficients reflects itself in rendering s_0 rather imprecise. Adding the stated errors in quadrature, we estimate in the SM [fixing m_b while varying μ and $\alpha_s(m_Z)$]:

$$s_0 = 2.88^{+0.44}_{-0.28}\ \text{GeV}^2. \tag{5.6}$$

The actual dilepton mass distributions and the FB asymmetry for the decays of interest in the SM will be given later, together with the corresponding estimates in some variants of SUSY.

VI. THE DECAYS $B\to(K,K^*)l^+l^-$ IN SUSY MODELS

First studies of rare B decays $B\to X_s\gamma$ and $B\to X_s l^+l^-$ in the context of MSSM were carried out in [16–18].[4] Since then, these studies have been updated by taking into account progress in theory and experiments. We employ the following models to study the rare $B\to K^{(*)}l^+l^-$ decays: (i) minimal supergravity (MSUGRA), (ii) relaxed SUGRA (RSUGRA), obtained from MSUGRA by relaxing the universal scalar mass condition at the GUT scale [19,20,22], (iii) minimal flavor violating supersymmetric model (MFV) (in the sense that the flavor violation is solely due to the standard CKM mechanism and resides in the charged current sector) [21], and (iv) the mass insertion approximation (MIA) [23]. The last of these models serves as a generic supersymmetric extension of the SM having non-CKM flavor violations. We do not consider models with broken R-parity and assume that there are no new phases from *new physics* beyond the SM, or, equivalently, that the constraints from the electric dipole moments of the neutron and charged lepton and indirect constraints from the decay $B\to X_s\gamma$ as well as other FCNC processes render these phases innocuous. This covers an important part of the supersymmetric parameter space, but not all. The issue of supersymmetric phases having measurable consequences in CP violations in B and K decays and electric dipole moments (EDMs) of the neutron and charged lepton is still far from being settled. As we have not studied CP asymmetries in the decays $B\to(K,K^*)l^+l^-$, the neglect of additional CP phases is not crucial to the analysis of the decay rates being presented here.

The strongest constraint on the minimal supersymmetric standard model (MSSM) parameter space is coming from data on $B\to X_s\gamma$ [7], given in Eq. (1.1). In terms of the Wilson coefficients, this puts a bound on the modulus of C_7^{eff}, given in Eq. (1.2) in the NLO approximation. The SM-based estimate of C_7^{eff} in the NLO precision is well within this range, which then restricts the otherwise allowed parameter space in the supersymmetric models we are considering. To be consistent with the precision of other contributions in $B\to X_s l^+l^-$, and for comparison with the rates and distributions in the SM, we work with $C_7^{\text{eff}}(m_{b,pole})$ in the LLA accuracy. This yields the bounds (at 95% C.L.)

$$0.249 \leqslant |C_7^{eff,LLA}(\mu=4.8\ \text{GeV})| \leqslant 0.374. \tag{6.1}$$

We remind at the outset that the theoretical uncertainties in the decay rates are estimated by us to be typically $\pm 35\%$. Hence SUSY searches in $B\to(K,K^*)l^+l^-$ will be unambiguous only for *drastic* SUSY effects.

To illustrate generic SUSY effects in $B\to(K,K^*)l^+l^-$, we start by assuming $|C_7^{\text{eff}}|\simeq|C_{7SM}^{\text{eff}}|$ allowing for two possible solutions, $C_7^{\text{eff}}<0$ (SM-like) and $C_7^{\text{eff}}>0$ (allowed in SUSY models). We also fix the other two coefficients C_9 and C_{10} to their respective SM values. We show the dilepton invariant mass distributions for $B\to K\mu^+\mu^-$ and $B\to K^*\mu^+\mu^-$ decays in Figs. 4 and 5(a), respectively. The FB asymmetry for $B\to K^*\mu^+\mu^-$ is shown in Fig. 5(b). These figures present a comparative study of the SM- and SUSY-based distributions, and the attendant theoretical uncertainties associated with the long-distance effects. For the latter, we have used the Krüger-Sehgal (KS) approach [29] and the Ali-Mannel-Morozumi (AMM) approach [28] to estimate the resonance-related uncertainties. These figures illustrate that despite non-perturbative uncertainties, it will be possible to distinguish between the SM and a theoretical scenario in which the magnitude of the effective coefficients are similar, but C_7^{eff} has the ''wrong sign.'' For the dilepton invariant mass, this reverses the sign of the interference term involving $\text{Re}((C_7^{\text{eff}})^*\cdot C_9^{\text{eff}})$ which leads to significant difference in the decays $B\to K^*l^+l^-$. More striking deviation from the SM prediction is found in A_{FB} for the models in which the condition Eq. (4.35) is not satisfied, resulting in a FB asymmetry which remains negative below the J/ψ-resonance region. This would be a *drastic deviation* from the SM, which cannot be fudged away due to non-perturbative effects. Interestingly, the situation $C_7^{\text{eff}}\simeq -C_{7SM}^{\text{eff}}$ is met in a number of SUSY models as discussed below. In addition, in a gen-

[4]There is a wrong sign in the chargino and neutralino box matching condition in [16]. This sign discrepancy between [16] and [18] has already been mentioned by the latter. We are grateful to T. Goto and F. Krüger for clarifying this point.

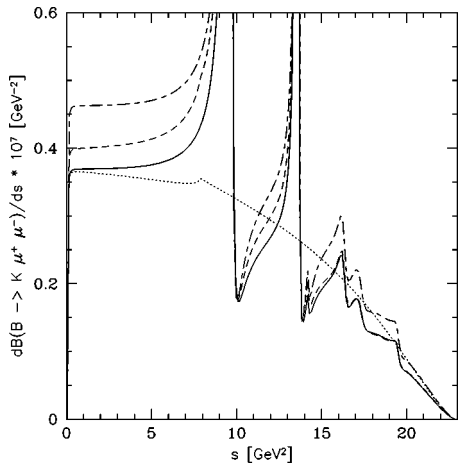

FIG. 4. The dilepton invariant mass distribution in $B \to K\mu^+\mu^-$ decays, using the form factors from LCSR as a function of s. Solid curve: SD + LD using Ref. [29]; dashed curve: SD + LD using Ref. [28]; dotted curve: pure SD; long-short dashed curve: SD + LD using Ref. [29] with $C_7^{\rm eff} = -C_{7SM}^{\rm eff}$.

eral flavor-violating supersymmetric model, also the other two Wilson coefficients (C_9 and C_{10}) may have either sign. In this case, the FB asymmetry in $B \to K^* l^+ l^-$ may have a functional dependence on the dilepton mass which is characteristically different than the ones obtaining in the SM and SUGRA models, as shown below.

More elaborate changes from new physics (NP) in the values of the relevant Wilson coefficients can be taken into account by the (correlated) ratios ($i = 7,9,10$)

$$R_i(\mu) \equiv \frac{\mathcal{C}_i^{NP} + \mathcal{C}_i^{SM}}{\mathcal{C}_i^{SM}} = \frac{\mathcal{C}_i}{\mathcal{C}_i^{SM}}, \tag{6.2}$$

which depend on the renormalization scale (except for C_{10}), for which we shall always take $\mu = m_{b,pole}$. The experimental constraint from $B \to X_s\gamma$ given in Eq. (1.1) now translates into the bound

$$0.80 < |R_7(\mu = 4.8\ \ {\rm GeV})| < 1.20, \tag{6.3}$$

where the coefficients are understood to be calculated in the leading-log approximation (LLA) precision. In the numerical estimates, we have used $\mathcal{B}_{sl} = (10.4 \pm 0.4)\%$ for the average semileptonic branching ratio, and have set the heavy quark expansion parameters to the values $\lambda_1 = -0.20\ {\rm GeV}^2$ and $\lambda_2 = 0.12\ {\rm GeV}^2$. The allowed values of the other two ratios R_9 and R_{10} are taken from the literature for the MSUGRA and RSUGRA models [20,22], and for the other two models, MFV and MIA, we have calculated them. In particular, in the MIA approach, large enhancements are anticipated in the branching ratio $\mathcal{B}(B \to X_s l^+ l^-)$ in some allowed region of the parameter space [23]. These enhancements, suitably modified by the form factors, are also present in the branching ratios for the exclusive decays $B \to (K, K^*) l^+ l^-$. However, as shown in Fig. 3, some of these branching ratios are bounded quite stringently, in particular, for the decays $B \to K^* e^+ e^-$ and $B \to K^* \mu^+ \mu^-$ [34,35]. Assuming R_7 in the allowed range, we shall work out the constraints on the effective coefficients C_9 and C_{10} (equivalently R_9 and R_{10}). Based on this analysis, we shall show the dilepton invariant mass spectra and the FB asymmetry in some representative cases.

A. $B \to (K, K^*) l^+ l^-$ in SUGRA models

We shall consider here both the minimal and restricted SUGRA models (MSUGRA, RSUGRA). The parameter space of these models may be decomposed into two qualitatively different regions, which can be characterized by $\tan\beta$ values. For small $\tan\beta$, say $\tan\beta \sim 2$, the sign of $C_7^{\rm eff}$ is the same as in the SM. Here, no spectacular deviations from the SM can be expected in the decays $B \to (K, K^*) l^+ l^-$. Given the theoretical uncertainties shown earlier by us, we think that it would be very difficult to disentangle any SUSY effects for this scenario in these decays. For large $\tan\beta$, the situation is more interesting due to correlations involving the branching ratio for $B \to X_s\gamma$, the mass of the lightest CP-even Higgs boson, m_h, and sign(μ_{susy}), appearing in the Higgs superpotential. In this case, there are two branches for the solutions for m_h and $\mathcal{B}(B \to X_s\gamma)$. The interesting scenario for SUSY searches in $B \to (K, K^*) l^+ l^-$ is the one in which sign(μ_{susy}) and m_h admit $C_7^{\rm eff}$ to be positive. For example, this happens for $\tan\beta \gtrsim 10$, in which case m_h

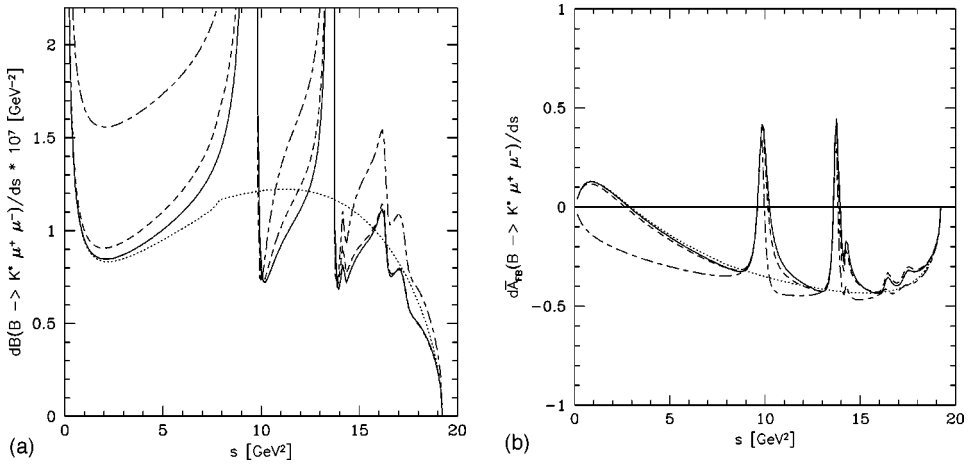

FIG. 5. The dilepton invariant mass distribution (a), and the normalized FB asymmetry (b) in $B \to K^* \mu^+ \mu^-$ decays, using the form factors in LCSR as a function of s in the SM. Solid curves: SD + LD according to Ref. [29]; dashed curves: SD + LD using Ref. [28]; dotted curves: pure SD; long-short dashed curves: SD + LD using Ref. [29] with $C_7^{\rm eff} = -C_{7SM}^{\rm eff}$.

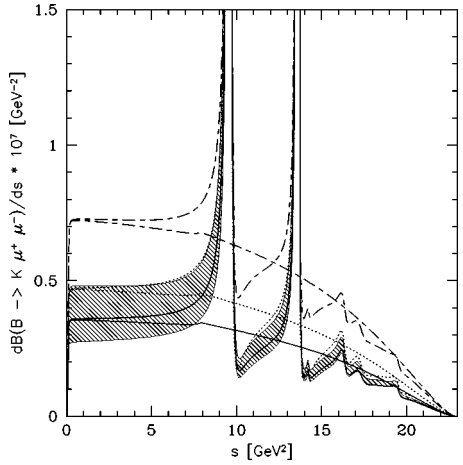

FIG. 6. The dilepton invariant mass distribution in $B\to K\mu^+\mu^-$ decays, using the form factors from LCSR as a function of s. All resonant $c\bar{c}$ states are parametrized as in Ref. [29]. The solid line represents the SM and the shaded area depicts the form factor–related uncertainties. The dotted line corresponds to the SUGRA model with $R_7=-1.2$, $R_9=1.03$ and $R_{10}=1$. The long-short dashed lines correspond to an allowed point in the parameter space of the MIA-SUSY model, given by $R_7=-0.83$, $R_9=0.92$ and $R_{10}=1.61$. The corresponding pure SD spectra are shown in the lower part of the plot.

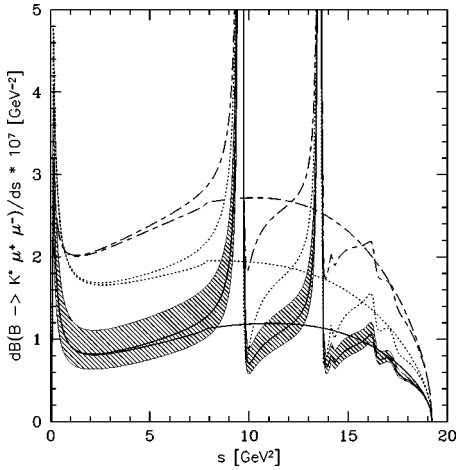

FIG. 7. The dilepton invariant mass distribution in $B\to K^*\mu^+\mu^-$ decays, using the form factors from LCSR as a function of s. All resonant $c\bar{c}$ states are parametrized as in Ref. [29]. The legends are the same as in Fig. 6.

$=(115-125)$ GeV and $C_7^{\rm eff}$ is positive and obeys the $B\to X_s\gamma$ bounds [22]. Following the generic case shown earlier, one expects a constructive interference of the terms depending on $C_7^{\rm eff}$ and C_9 in the dilepton invariant mass spectra. For the sake of illustration, we use

$$R_7=-1.2,\quad R_9=1.03,\quad R_{10}=1.0, \tag{6.4}$$

obtained for $\tan\beta=30$ [20], as a representative large-$\tan\beta$ solution, to study the effects on our observables. We find that in the low-q^2 region the branching ratio for $B\to K\mu^+\mu^-$ is enhanced by about 30% compared to the SM one, as shown in Fig. 6. This enhancement is difficult to disentangle from the non-perturbative uncertainties attendant with the SM distributions (shown as the shaded band in this figure). The dilepton mass distribution for $B\to K^*\mu^+\mu^-$ is more promising, as in this case the enhancement is around 100%, see Fig. 7, and this is distinguishable from the SM-related theoretical uncertainties (shown as the shaded band in this figure). Note that the resulting branching ratios are consistent with the present experimental upper bounds on these decays given earlier. The supersymmetric effects presented here are very similar to the ones worked out for the inclusive decays $B\to X_s l^+l^-$ [20], where enhancements of $(50-100)\%$ were predicted in the low-q^2 branching ratios. The effect of R_7 being negative is striking in the FB asymmetry as shown in Fig. 8, in which the two SUGRA curves are plotted using Eq. (6.4) (for $R_7<0$) and by flipping the sign of R_7 but keeping the magnitudes of R_i to their values given in this equation. Summarizing for the SUGRA theories, large $\tan\beta$ solutions lead to $C_7^{\rm eff}$ being positive, which implies that FB asymmetry below the J/ψ-resonant region remains negative (hence, no zero in the FB asymmetry in this region) and one expects an enhancement up to a factor two in the dilepton mass distribution in $B\to K^*e^+e^-$ and $B\to K^*\mu^+\mu^-$.

B. $B\to(K,K^*)l^+l^-$ in MFV-SUSY model

The MFV-SUSY model is based on the assumption of minimal flavor violation. Here, quarks and squarks are aligned so there is no flavor-changing $q-\tilde{q}'-(\tilde{Z},\tilde{\gamma},\tilde{g})$ vertex and the charged one, $d-\tilde{u}-\tilde{\chi}^{\pm}$, is governed by the

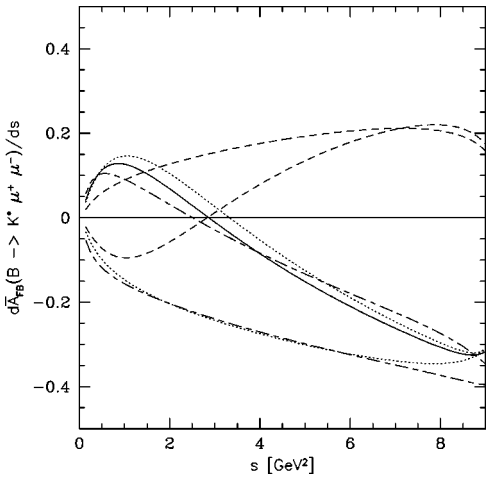

FIG. 8. The normalized forward-backward asymmetry in $B\to K^*\mu^+\mu^-$ decay as a function of s, using the form factors from the LCSR approach. All resonant $c\bar{c}$ states are parametrized as in Ref. [29]. The solid line denotes the SM prediction. The dotted (long-short dashed) lines correspond to the SUGRA (the MIA-SUSY) model, using the parameters given in Eq. (6.4) [Eq. (6.10)] with the upper and lower curves representing the $C_7^{\rm eff}<0$ and $C_7^{\rm eff}>0$ case, respectively. The dashed curves indicating a positive asymmetry for large s correspond to the MIA-SUSY models using the parameters given in Eq. (6.11), i.e. the ''best depression scenario'' with $C_{10}>0$.

CKM matrix. As a consequence, in this model neutralino-down-squark and gluino-down-squark graphs do not contribute to either $b\to s\gamma$ or $b\to s l^+ l^-$ transitions. In addition to the charged Higgs-boson–top-quark graphs, chargino-up type squarks loops with a light stop $\tilde{t}_1$, and the $W^\pm$-top quark loops, present in the SM, give the dominant contribution. While not holding generally, the assumptions in the minimal flavor violation (MFV) SUSY model are valid over an important part of the minimal supersymmetric parameter space [21]. They have the simplifying feature that the dominant supersymmetric effects remain confined to charged current transitions and relatively easy to test experimentally due to well-defined correlations in several measurable quantities involving FCNC transitions [21,12].

As is well known [72], in the two-Higgs doublet model of type II (2HDM model II), which is embedded also in the MFV-SUSY construct, the charged-Higgs-boson contribution is always additive to the SM, i.e., $C_7^{\rm eff}(\text{2HDM})<0$, yielding a lower bound on the charged Higgs boson mass $m_{H^\pm}$ (almost) independent of $\tan\beta$, above $\tan\beta>1$. In MFV, the $\tilde{\chi}^\pm-\tilde{t}_1$ loop can compensate the $H^\pm-t$ contribution, with a large positive contribution to $C_7^{\rm eff}$. We scan over the parameter space in the range 55 GeV$<m_{H^\pm}<1$ TeV, $0<M_2,|\mu_{susy}|<500$ GeV, where μ_{susy} is the bilinear Higgs boson coupling in the superpotential and M_2 is the gaugino soft breaking mass. We use $m_{\tilde{q}}=m_{\tilde{t}_2}=1$ TeV, where $m_{\tilde{q}}$ denotes the (degenerate) masses of other than top squarks, and fix $m_{\tilde{\nu}}=50$ GeV to its lower bound. We reject too light charginos, demanding $m_{\tilde{\chi}^\pm}>70$ GeV, and also solutions which do not satisfy the bounds from the branching ratio on $B\to X_s\gamma$. The chargino contribution to $C_7^{\rm eff}$ decreases for larger values of $m_{\tilde{t}_1}$ and we therefore keep it to its minimal value $m_{\tilde{t}_1}=70$ GeV. We have chosen a stop mixing angle $\theta_{\tilde{t}}=\pm 2\pi/5$, i.e. the light stop $\tilde{t}_1=\cos\theta_{\tilde{t}}\tilde{t}_L+\sin\theta_{\tilde{t}}\tilde{t}_R$ is almost right handed.

For small $\tan\beta$, for which we again take $\tan\beta=2$, we find that the ratio R_7 remains positive, i.e. $C_7^{\rm eff}<0$, and lies within the experimentally allowed bounds from $B\to X_s\gamma$, and the other two ratios are in the range $0.98<R_9<1.07$ and $0.79<R_{10}<1.15$. For large $\tan\beta$, taken to be 30, just as in the SUGRA models discussed earlier, $C_7^{\rm eff}$ changes sign ($R_7<0$). The ratios R_9 and R_{10} are again always positive but now R_9 is almost identical to 1, and R_{10} tends to lie below the SM value. Numerically, we find the ranges $0.99<R_9<1$, $0.93<R_{10}<1.02$. The maximal (minimal) value of $\tan\beta$ found for $R_7>0(<0)$ is 5 (20). In contrast, a no mixing choice $\theta_{\tilde{t}}=\pm\pi/2$ or $\tilde{t}_1\simeq\tilde{t}_R$ yields, for both $\tan\beta=2$ and 30, $C_7^{\rm eff}<0$ or equivalently $R_7>0$.

In general, in the MFV model, SUSY effects on C_9 and C_{10} are much smaller than the corresponding one on $C_7^{\rm eff}$. A large value of $\tan\beta$ helps $C_7^{\rm eff}$ to satisfy the $B\to X_s\gamma$ bounds but admits a sign opposite to the one in the SM. Dominant SUSY contributions to C_9 and C_{10} are due to the charged Higgs boson exchange and are suppressed as $\sim 1/\tan^2\beta$, for large $\tan\beta$. Chargino effects in C_9 and C_{10} increase for larger values of the ratio $M_2/|\mu_{susy}|>1$. Using the central values of the parameters and the LCSR form factors, the maximal non-resonant branching ratios in the MFV are found for the ratios $R_7=-1.2$, $R_9=1.0$ and $R_{10}=1.02$: $\mathcal{B}_{nr}^{maxMFV}(B\to K\mu^+\mu^-)=7.5\times10^{-7}$ and $\mathcal{B}_{nr}^{maxMFV}(B\to K^*\mu^+\mu^-)=3.2\times10^{-6}$. While larger than the corresponding branching ratios in the SM, they are compatible with the present experimental bounds [34,35]. Our findings in the MFV-SUSY model are very similar to the SUGRA case and in agreement with [19] for the inclusive decays. As the values of R_i for the maximal non-resonant branching ratios in the MFV model are almost identical to their SUGRA-model counterparts given in Eq. (6.4), for which we have shown the dilepton invariant mass spectra and FB asymmetry, we refrain from showing the corresponding figures for the MFV case.

C. $B\to(K,K^*)l^+l^-$ in the MIA approach

The minimal insertion approach aims at including all possible squark mixing effects in a model independent way. Choosing a $q,\tilde{q}$ basis where the $q-\tilde{q}-\tilde{\chi}^0$ and $q-\tilde{q}-\tilde{g}$ couplings are flavor diagonal, flavor changes are incorporated by a non-diagonal mass insertion in the $\tilde{q}$ propagator, which can be parametrized as ($A,B=$ left, right) [73]

$$(\delta_{ij}^{up,down})_{A,B}=\frac{(m_{ij}^{up,down})^2_{A,B}}{m_{\tilde{q}}^2}, \tag{6.5}$$

where $(m_{ij}^{up,down})^2_{A,B}$ are the off-diagonal elements of the up-(down) squark mass squared matrices that mix flavor i and j, for both the right- and left-handed scalars, and $m_{\tilde{q}}^2$ is the average squark mass squared. The sfermion propagators are expanded in terms of the δs. The Wilson coefficients have the following structure ($k=7,9,10$):

$$\mathcal{C}_k=\mathcal{C}_k^{SM}+\mathcal{C}_k^{diag}+\mathcal{C}_k^{MIA}, \tag{6.6}$$

where $\mathcal{C}^{MIA}$ is given in terms of $(\delta_{ij}^{up,down})^2_{A,B}$ up to two mass insertions [23], and $\mathcal{C}_k^{diag}$ being the SUSY contribution in the basis where only flavor-diagonal contributions are allowed. It is tacitly assumed that the δs are small and this defines the theoretical consistency of this approach which has to be checked *a posteriori*.

The MIA-SUSY approach has been recently used in the analysis of the decays $B\to X_s l^+ l^-$ [23], taking into account the present bounds on the coefficient $C_7^{\rm eff}(m_B)$ following from the decay $B\to X_s\gamma$. The other two coefficients $\mathcal{C}_9^{MIA}$ and $\mathcal{C}_{10}^{MIA}$ are calculated by scanning over the allowed supersymmetric parameter space [23]. For $\mu_{susy}\simeq-160$ GeV, $m_{\tilde{g}}\simeq m_{\tilde{q}}\simeq250$ GeV, $m_{\tilde{t}_1}=90$ GeV, $m_{\tilde{\nu}}\simeq50$ GeV, these coefficients are expressed as

$$\mathcal{C}_9^{MIA}(m_B)=-1.2(\delta_{23}^u)_{LL}+0.69(\delta_{23}^u)_{LR}-0.51(\delta_{23}^d)_{LL},$$
$$\mathcal{C}_{10}^{MIA}=1.75(\delta_{23}^u)_{LL}-8.25(\delta_{23}^u)_{LR}. \tag{6.7}$$

Of these, the mass insertions $(\delta_{23}^d)_{LL}$ and $(\delta_{23}^u)_{LL}$ are related by a CKM rotation and the bound on one implies a similar bound on the other. One may have marked enhancement or

depletion in the branching ratios for the decay $B\to X_s l^+ l^-$. Note also the large numerical coefficient of $(\delta^u_{23})_{LR}$ in the expression for $\mathcal{C}_{10}^{MIA}$. For the parameters for which Eq. (6.7) holds, the diagonal-SUSY contributions to C_9 and C_{10} are: $C_9^{diag}(m_B)=-0.35$, $C_{10}{}^{diag}=-0.27$. Depending on the value of $(\delta^u_{23})_{LR}$ and $(\delta^u_{23})_{LL}$, the coefficient $\mathcal{C}_{10}^{MIA}$ may easily overcome the SM and the diagonal-MSSM contributions in this coefficient, changing the overall sign of the FB asymmetry. This feature is a marked difference between this scenario and the competing ones, namely SUGRA and MFV, where C_{10} remains close to the SM value (see Table I). This feature has been noted already in [23] in the context of the FB asymmetry in the inclusive decay $B\to X_s l^+ l^-$.

To maximize the effects in this general flavor-violating supersymmetric context, several special cases have been studied in Ref. [23] in detail. We shall discuss the following three scenarios from this work:[5]

(1) ''Best enhancement scenario'' for the branching ratio $\mathcal{B}(B\to X_s l^+ l^-)$, which corresponds to the choice $C_7{}^{\rm eff}=0.445$, $(\delta^d_{23})_{LL}=(\delta^u_{23})_{LL}=-0.5$ and $(\delta^u_{23})_{LR}=0.9$;

(2) ''Best enhancement scenario with $C_7{}^{\rm eff}<0$,'' corresponding to using $C_7{}^{\rm eff}=-0.445$, $(\delta^d_{23})_{LL}=-0.5$, $(\delta^u_{23})_{LL}=-0.1$ and $(\delta^u_{23})_{LR}=0.9$;

(3) ''Best depression scenario,'' corresponding to $C_7{}^{\rm eff}=-0.25$, $(\delta^d_{23})_{LL}=0.5$, $(\delta^u_{23})_{LL}=0.1$ and $(\delta^u_{23})_{LR}=-0.6$.

With these choices, drastic effects in the branching ratios and the FB asymmetry have been predicted for the decays $B\to X_s l^+ l^-$, as displayed in Figs. 5–8 in Ref. [23]. To wit, in the first scenario listed above, enhancements as large as a factor 5 are admissible in $\mathcal{B}(B\to X_s e^+ e^-)$ and even higher, 6.5, in $B\to X_s\mu^+\mu^-$.

We shall largely follow this analysis here in discussing the decay characteristics of the exclusive decays $B\to(K,K^*)l^+l^-$ but would like to add a dissenting remark concerning the coefficient $C_7{}^{\rm eff}(m_B)$. We recall that the extremal values used for $C_7{}^{\rm eff}(m_B)$ in [23] correspond to using the 99% C.L. limits on $\mathcal{B}(B\to X_s\gamma)$, which give the bounds $0.252<|C_7{}^{\rm eff}|<0.445$ in the NLO approximation. This procedure allows a much larger range for the ratio R_7 than the one given in Eq. (6.3), which is then partly reflected in the branching ratios for $B\to X_s l^+ l^-$.

We argue that even with this more restricted range of $C_7{}^{\rm eff}$, the two ''best enhancement scenarios for $B\to X_s l^+ l^-$'' of Ref. [23] alluded to above give too large branching ratios for the exclusive decays being studied here. To be specific, in the first scenario, the parameters given above translate into $R_9=1.26$ and $R_{10}=2.84$.[6] The central values of the form factors calculated here in the LCSR approach then lead to the following branching ratio:

TABLE VII. Coefficients of the nonresonant branching ratio $\mathcal{B}(B\to K^*\mu^+\mu^-)$ in units of 10^{-7} in the decomposition as in Eq. (6.9), integrated over the full q^2 range for different sets of form factors given in Tables III–V.

	$a^{(nr)}_{K^*}$	$b^{(nr)}_{K^*}$	$c^{(nr)}_{K^*}$	$d^{(nr)}_{K^*}$	$e^{(nr)}_{K^*}$	$f^{(nr)}_{K^*}$	$g^{(nr)}_{K^*}$
FF(central)	21.295	0.502	0.500	3.530	1.434	0.413	0.148
FF(max)	28.183	0.630	0.633	4.577	1.859	0.520	0.183
FF(min)	16.795	0.417	0.416	2.864	1.164	0.343	0.125

$\mathcal{B}^{max,MIA}_{nr}(B\to K^*\mu^+\mu^-)=11.5\times10^{-6}$, which is approximately 3 times larger than the recent CDF (90% C.L.) upper limit on this quantity [34],

$$\mathcal{B}(B^0\to K^{*0}\mu^+\mu^-)<4.0\times10^{-6}. \tag{6.8}$$

The $B\to K$ transition in this scenario is likewise enhanced, yielding a branching ratio $\mathcal{B}^{max,MIA}_{nr}(B\to K\mu^+\mu^-)=3.2\times10^{-6}$, which is typically a factor 5 larger than the SM branching ratio, but still compatible with the experimental upper limit, $\mathcal{B}(B^+\to K^+\mu^+\mu^-)<5.2\times10^{-6}$ [34]. Hence, the present experimental upper bound on $B\to K^*\mu^+\mu^-$ provides non-trivial bounds on C_9 and C_{10}, equivalently on R_9 and R_{10}, which we now proceed to work out.

D. Bounds on C_9 and C_{10} from present data

The branching ratios $B\to(K,K^*)l^+l^-$ can be expressed as quadratic equations in the coefficients $C_7{}^{\rm eff}$, C_9 and C_{10}. Given the branching ratios (equivalently upper bounds), these equations can be solved numerically and yield the allowed contours in the C_9-C_{10} plane. For working out the constraints, we use the experimental bound in Eq. (6.8) and the following expression which follows from Eq. (4.27):

$$\begin{aligned}\mathcal{B}(B\to K^*\mu^+\mu^-)=&\,a^{(nr)}_{K^*}|C_7{}^{\rm eff}|^2+b^{(nr)}_{K^*}|C_9|^2+c^{(nr)}_{K^*}|C_{10}|^2\\&+d^{(nr)}_{K^*}C_7{}^{\rm eff}C_9+e^{(nr)}_{K^*}C_7{}^{\rm eff}+f^{(nr)}_{K^*}C_9\\&+g^{(nr)}_{K^*}.\end{aligned} \tag{6.9}$$

The coefficients $a^{(nr)}_{K^*},\ldots,g^{(nr)}_{K^*}$ are tabulated in Table VII, using the central values of the $B\to K^*$ form factors in Table III and the maximum and minimum values of the same given in Tables IV and V, respectively. Of these, the coefficients $b^{(nr)}_{K^*}$ and $c^{(nr)}_{K^*}$ coincide if one neglects the $l^\pm$ masses. The superscript on these coefficients is a reminder that only nonresonant contributions are included.

The quadratic equation in Eq. (6.9) is solved numerically for the two distinct situations $C_7{}^{\rm eff}<0$ (SM-like) and $C_7{}^{\rm eff}>0$ (new physics scenario) in the experimentally allowed range for $C_7{}^{\rm eff}$ given in Eq. (6.1). The resulting 90% C.L. allowed contours are shown in Fig. 9 and Fig. 10, respectively. The solid curves in these figures are obtained by using the central values of the form factors and the inner and outer dashed curves represent the maximal and minimal allowed values of the same, respectively. Note that the loosest bounds emerge from the minimal allowed values of the form factors.

[5]The specific values given above for the mass insertion parameter $(\delta^d_{23})_{LL}$ have been kindly provided to us by Ignazio Scimemi. We also draw attention to several misprints in the tables given in [23] and trust that an Erratum is being issued by the authors of Ref. [23].

[6]We neglect the effect from the RG running from $\mu=m_B$ (used in [23]) to $\mu=m_{b,pole}$ used by us.

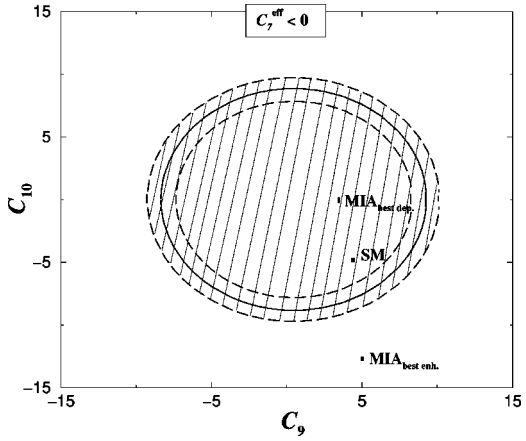

FIG. 9. Bounds on the coefficients $C_9(m_B)$ and C_{10} resulting from the experimental upper bound $\mathcal{B}(B^0 \to K^{*0}\mu^+\mu^-) < 4.0 \times 10^{-6}$ (at 90% C.L.) [34] and $C_7^{\rm eff}(\mu = 4.8\ {\rm GeV}) = -0.249$ from the bounds given in Eq. (6.1).The SM point and two representative points in the SUSY-MIA approach from Ref. [23] are also shown. The three curves correspond to using the central values of the form factors (solid curve), the minimum (outer dashed curve) and maximum (inner dashed curve) allowed values discussed in Sec. III.

Also, in working out the constraints shown in these figures, we have fixed $|C_7^{\rm eff}| = |C_{7min}^{\rm eff}| = 0.249$ in the allowed range given in Eq. (6.1), as this gives for both the cases ($C_7^{\rm eff} < 0$ and $C_7^{\rm eff} > 0$) the loosest bounds on C_9 and C_{10}. This can be seen in Fig. 11 and Fig. 12 drawn for $C_7^{\rm eff} < 0$ and $C_7^{\rm eff} > 0$, respectively, where we show the dependence of the bounds in the C_9-C_{10} plane on the experimentally allowed range for $|C_7^{\rm eff}|$ given in Eq. (6.1). In these figures, we use the minimum values of the form factors given in Table V for reasons given above. In Figs. 9 and 11, we also show the SM point (see Table I) and the SUSY-MIA points for the ''best enhancement scenario with $C_7^{\rm eff} < 0$,'' corresponding to $C_9(m_B) = 5.0$, $C_{10} = -12.5$, and the ''best depression scenario with $C_7^{\rm eff} < 0$,'' corresponding to $C_9(m_B) = 3.2$, $C_{10} = 0.2$ [23]. We note that the ''best enhancement scenario with $C_7^{\rm eff} < 0$'' is ruled out by data. The other MIA-SUSY point, as well as the SM, are both well within the experimental bound. The SUSY-MIA point corresponding to the ''best enhancement scenario with $C_7^{\rm eff} > 0$'' of Ref. [23] is shown in the C_9-C_{10} plane in Figs. 10 and 12. This corresponds to the point $C_9(m_B) = 5.5$, $C_{10} = -13.2$. As anticipated, this ''best enhancement scenario with $C_7^{\rm eff} > 0$'' is convincingly ruled out by the experimental upper bound on $\mathcal{B}(B \to K^*\mu^+\mu^-)$. The analysis shown in Figs. 9–12 holds for all models discussed here in this paper in which the SD physics can be encoded in terms of the three real Wilson coefficients $C_7^{\rm eff}$, C_9 and C_{10}. The point we wish to stress is that existing data on $B \to K^*\mu^+\mu^-$, in conjunction with the branching ratio $\mathcal{B}(B \to X_s\gamma)$, provides non-trivial constraints on C_9 and C_{10}.

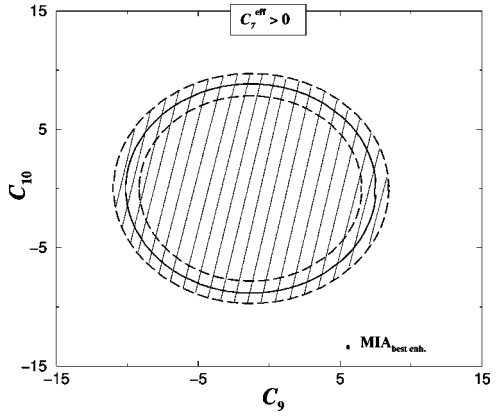

FIG. 10. The same as Fig. 9 but for the solution with $C_7^{\rm eff} = 0.249$. The point MIA_{best} corresponds to the ''best enhancement scenario'' of Ref. [23], discussed in the text.

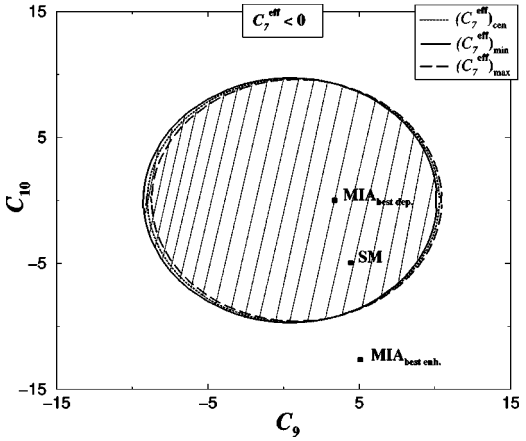

FIG. 11. The same as Fig. 9, but showing the dependence of the bounds on the experimentally allowed range for $|C_7^{\rm eff}|$, $0.249 \leqslant |C_7^{\rm eff}| \leqslant 0.374$, with the form factors fixed to their minimum values given in Table V.

Illustrative examples of the dilepton invariant mass spectrum in the decays $B \to K\mu^+\mu^-$ and $B \to K^*\mu^+\mu^-$ in the MIA approach are shown in Figs. 6 and 7, respectively. They have been calculated for the following values:

$$R_7 = \pm 0.83, \quad R_9 = 0.92, \quad R_{10} = 1.61, \qquad (6.10)$$

which are allowed by the present experimental bounds. The

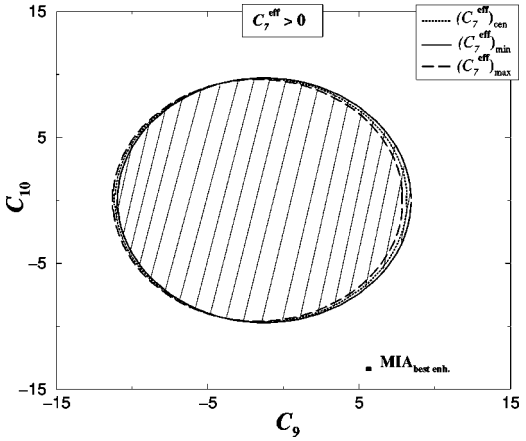

FIG. 12. The same as Fig. 11, but with $C_7^{\rm eff} > 0$.

TABLE VIII. Coefficients in units of 10^{-7} defined in Eqs. (6.13) and (6.14) in the KS prescription [29].

	a	b	c	d	e	f	g	h	j	k
K	0.193	0.068	0.068	0.230	0.163	0.097	0.045	-	-	-
K^*	13.119	0.197	0.196	1.760	0.995	0.236	0.083	0.943	0.089	0.061

characteristic difference in this case, as compared to the SUGRA and MFV-SUSY models, lies in the significantly enhanced value of C_{10}.

As already mentioned, a characteristic of the MIA approach is that the sign of C_{10} ($C_{10}^{SM}<0$) depends on the quantities $(\delta_{23}^u)_{LR}$ and $(\delta_{23}^u)_{LL}$. In particular, the large number in front of $(\delta_{23}^u)_{LR}$ in C_{10}, obtained for the specific values of the SUSY parameter space, could change the sign of this Wilson coefficient. This has no effect on the dilepton invariant mass distributions, as they depend quadratically on C_{10}, but it would change the sign of A_{FB} in $B\to K^*l^+l^-$. To illustrate this, we use the parameters close to the so-called ''best depression'' scenario [23], corresponding to the following values:

$$R_7=\pm 0.83, \quad R_9=0.79, \quad R_{10}=-0.38, \tag{6.11}$$

and plot the resulting normalized FB asymmetry in Fig. 8. The positive FB asymmetry in $B\to K^*l^+l^-$ (as well as in $B\to X_s l^+l^-$ shown in [23]) for the dilepton invariant mass below the resonant J/ψ region is rather unique, as none of the other models considered here (SM, SUGRA and MFV) admit solutions with positive C_{10}.

Finally, to facilitate a model independent determination of the coefficients ${C_7}^{\rm eff}$, C_9, and C_{10} from the decays $B\to(K,K^*)l^+l^-$, we write down a parametrization of the partially integrated branching ratios and FBA in the low s region. Using, for the sake of definiteness, $s_{min}=0.25$ GeV^2, $s_{max}=8.0$ GeV^2, the partial branching ratios $\Delta\mathcal{B}_X$ and the corresponding FB asymmetry $\Delta\mathcal{A}_{FB}$ can be expressed as ($X=K,K^*$)

$$\Delta\mathcal{B}_X\equiv\int_{s_{min}}^{s_{max}}{\rm d}s\,\frac{{\rm d}\mathcal{B}(B\to X\mu^+\mu^-)}{{\rm d}s} \tag{6.12}$$

$$=a_X|{C_7}^{\rm eff}|^2+b_X|C_9|^2+c_X|C_{10}|^2+d_X{C_7}^{\rm eff}C_9 +e_X{C_7}^{\rm eff}+f_XC_9+g_X \tag{6.13}$$

$$\Delta\mathcal{A}_{FB}\equiv\tau_B\int_{s_{min}}^{s_{max}}{\rm d}s\frac{{\rm d}\mathcal{A}_{FB}(B\to K^*\mu^+\mu^-)}{{\rm d}s}$$

$$=C_{10}(h_X{C_7}^{\rm eff}+j_XC_9+k_X). \tag{6.14}$$

Numerical values of the coefficients are given in Table VIII. They have been obtained by using the central values of the form factors and other parameters given in Table III and Table VI, respectively. Specifying a model by the effective coefficients ${C_7}^{\rm eff}(m_B)$, ${C_9}^{\rm eff}(m_B)$ and C_{10} enables one to obtain readily the predictions for $\Delta\mathcal{B}_X$ and $\Delta\mathcal{A}$ in this model. In the SM, we estimate $\Delta\mathcal{B}_K=2.90\times10^{-7}$, $\Delta\mathcal{B}_{K*}=7.67\times10^{-7}$ and $\Delta\mathcal{A}_{FB}=-0.71\times10^{-7}$, yielding $\Delta\overline{\mathcal{A}}_{FB}=\Delta\mathcal{A}_{FB}/\Delta\mathcal{B}_{K*}=-9.2\%$. The branching ratios for the decays $B\to(K,K^*)e^+e^-$ are practically identical. Typical theoretical errors on these quantities, obtained by varying the form factors and the parameters m_t, m_b, μ and Λ_{QCD} in the ranges discussed earlier and adding the individual errors in quadrature are $\pm30\%$ for $\Delta\mathcal{B}$ and $\pm38\%$ for $\Delta\mathcal{A}$. However, the branching ratios and the FB asymmetry may be significantly enhanced (or depressed) in some variants of the supersymmetric models discussed. With $O(10^8)$ $B\overline{B}$ events anticipated at the B factories and HERA-B, and much higher yields at the Fermilab Tevatron and CERN LHC experiments, these rates and asymmetries will allow precision tests of the SM and may indicate the presence of new physics.

VII. SUMMARY AND CONCLUDING REMARKS

Before summarizing our results, we would like to comment on the contributions from the helicity-flipped counterparts of the SM operators $\mathcal{O}_7$, $\mathcal{O}_9$ and $\mathcal{O}_{10}$:

$$\mathcal{O}_7'=\frac{e}{16\pi^2}\overline{s}\sigma_{\mu\nu}m_bLbF^{\mu\nu}, \tag{7.1}$$

$$\mathcal{O}_9'=\frac{e^2}{16\pi^2}\overline{s_R}\gamma^\mu b_R\overline{l}\gamma_\mu l, \tag{7.2}$$

$$\mathcal{O}_{10}'=\frac{e^2}{16\pi^2}\overline{s_R}\gamma^\mu b_R\overline{l}\gamma_\mu\gamma_5 l. \tag{7.3}$$

In an enlarged operator basis including these and the SM operators, the various distributions for the decays of interest can be obtained from the substitutions $C_i\to C_i+C_i'$ ($i=7,9,10$) in the matrix elements and the auxiliary functions Eqs. (4.6)–(4.17) for $B\to K$, and for $B\to K^*$ in the terms which are proportional to the form factors V and T_1. In the remainder of the $B\to K^*$ amplitude, the contribution of the helicity-flipped operators enters with the opposite sign, i.e., $C_i\to C_i-C_i'$.

We note that in all models with minimal flavor violation, like the SM, 2HDM, and MFV, the contributions of the flipped operators $\mathcal{O}_{7,9,10}'$ vanish in the $m_s\to0$ limit. In the general non-diagonal MSSM scenarios, there are finite contributions even for a vanishing s-quark mass due to the neutralino-gluino-down-squark loops. However, under the assumption that no large cancellations happen, we can conclude from the data on $\mathcal{B}(B\to X_s\gamma)$ which bounds $|{C_7}^{\rm eff}|^2+|C_7^{\rm eff'}|^2$ that $C_7^{\rm eff'}$ must be small compared to ${C_7}^{\rm eff}$. Further, neglecting box diagrams, the helicity structure of the (penguin) loops responsible for $C_{9,10}'$ can be related to the ones of the flipped photon penguin $C_7^{\rm eff'}$ and hence is sup-

pressed as well. We also note that we have neglected the effects of the neutral Higgs exchanges, which may lead to some inaccuracies for the decay $B\to(K,K^*)\tau^+\tau^-$ in some parts of the SUSY parameter space. They are insignificant for the decays involving the $(K,K^*)\mu^+\mu^-$ and $(K,K^*)e^+e^-$ states, where most of the experimental searches will be concentrated.

We summarize our results: We have undertaken an improved calculation of the form factors in the decays $B\to(K,K^*)l^+l^-$ in the light cone QCD sum rule approach. Using this framework, we have calculated the partial branching ratios, dilepton invariant mass spectra and the forward-backward asymmetry for these decays in the context of the SM. We have also undertaken a comparative study of the phenomenological profiles of these decays in a number of supersymmetric models. These include the SUGRA models, minimal-flavor-violation SUSY model, and a general flavor-violating SUSY framework using the mass insertion approximation. The role of the forward-backward asymmetry in the decays $B\to K^*l^+l^-$ in searching for new physics is emphasized. We show that the large-$(\tan\beta)$ solution in the SUGRA models, but also some parameter space of the MIA model, yield FB asymmetries, which are strikingly different from the SM. In particular, the value of the dilepton invariant mass for which the FB asymmetry may become zero, s_0, may provide a precision test of the SM. A simple analytic expression for s_0 is derived, and we have argued that the form factor dependence in s_0 cancels in the large energy expansion approximation. We have analyzed the present data on $B\to X_s\gamma$ and existing limits on the decays $B\to(K,K^*)l^+l^-$ to put bounds on the coefficients C_9 and C_{10}. While these bounds do not yet probe the SM, they do provide non-trivial constraints on extensions of the SM. In particular, the ''best enhancement SUSY-MIA scenarios'' for the branching ratios $\mathcal{B}(B\to X_s l^+l^-)$, shown for some chosen supersymmetric parameters in Ref. [23], are ruled out by the existing upper limit on the exclusive branching ratio $\mathcal{B}(B^0\to K^{*0}\mu^+\mu^-)$ [34]. Finally, we show the dilepton mass spectra and the FB asymmetry for illustrative values of the supersymmetric parameters and argue that the decays $B\to(K,K^*)l^+l^-$ hold great promise in unraveling new physics.

ACKNOWLEDGMENTS

A.A. would like to acknowledge helpful communication with Ignazio Scimemi on the work reported in [23]. G.H. would like to thank Frank Krüger and Tilman Plehn for useful discussions, and the Fermilab theory group for the hospitality during her stay, where a part of this work has been done. P.B. is supported by the Deutsche Forschungsgemeinschaft (DFG) through the Heisenberg Program. L.T.H. would like to thank the Alexander von Humboldt Stiftung for financial support. This project is partially supported by the EEC-TMR Program, Contract N. FMRX-CT98-0169. This work was supported by the Department of Energy, Contract DE-AC03-76SF00515.

[1] S.L. Glashow, J. Iliopoulos, and L. Maiani, Phys. Rev. D **2**, 1285 (1970).
[2] N. Cabibbo, Phys. Rev. Lett. **10**, 531 (1963); M. Kobayashi and K. Maskawa, Prog. Theor. Phys. **49**, 652 (1973).
[3] A. Ali, C. Greub, and T. Mannel, in *Proceedings of the ECFA Workshop on a European B Meson Factory*, Hamburg, Germany, 1993, edited by R. Aleksan and A. Ali, Report DESY 93-016 (ZU-TH 4/93, IKDA 93/5).
[4] C.S. Kim, T. Morozumi, and A.I. Sanda, Phys. Rev. D **56**, 7240 (1997).
[5] A. Ali and G. Hiller, Eur. Phys. J. C **8**, 619 (1999).
[6] A. Ali, H. Asatrian, and C. Greub, Phys. Lett. B **429**, 87 (1998).
[7] CLEO Collaboration, M.S. Alam *et al.*, Phys. Rev. Lett. **74**, 2885 (1995); CLEO Collaboration, S. Ahmed *et al.*, CLEO CONF 99-10 (hep-ex/9908022).
[8] ALEPH Collaboration, R. Barate *et al.*, Phys. Lett. B **429**, 169 (1998).
[9] J. Alexander, in *Proceedings of the XXIXth International Conference on High Energy Physics*, Vancouver, Canada, 1998, edited by A. Astbury, D. Axen, and J. Robinson (World Scientific, Singapore, 1999).
[10] A. Ali, to be published in the Proceedings of the 7th International Symposium on Heavy Flavor Physics, Santa Barbara (CA), 1997, DESY 97-162 (hep-ph/9709507).
[11] A.J. Buras, TUM-HEP-316-98 (hep-ph/9806471); TUM-HEP-349-99 (hep-ph/9905437).
[12] A. Ali and D. London, Eur. Phys. J. C **9**, 687 (1999).
[13] S. Mele, Phys. Rev. D **59**, 113011 (1999).
[14] F. Parodi, P. Roudeau, and A. Stocchi, LAL-99-03 (hep-ex/9903063).
[15] Particle Data Group, C. Caso *et al.*, Eur. Phys. J. C **3**, 1 (1998).
[16] S. Bertolini *et al.*, Nucl. Phys. **B353**, 591 (1991).
[17] A. Ali, G.F. Giudice, and T. Mannel, Z. Phys. C **67**, 417 (1995).
[18] P. Cho, M. Misiak, and D. Wyler, Phys. Rev. D **54**, 3329 (1996).
[19] J.L. Hewett and J.D. Wells, Phys. Rev. D **55**, 5549 (1997).
[20] T. Goto *et al.*, Phys. Rev. D **55**, 4273 (1997); T. Goto, Y. Okada, and Y. Shimizu, *ibid.* **58**, 094006 (1998).
[21] M. Ciuchini *et al.*, Nucl. Phys. **B534**, 3 (1998).
[22] T. Gotou, Y. Okada, and Y. Shimizu, KEK-TH-611 (hep-ph/9908499).
[23] E. Lunghi *et al.*, hep-ph/9906286.
[24] S. Baek and P. Ko, Phys. Rev. Lett. **83**, 488 (1999); Phys. Lett. B **462**, 95 (1999).
[25] A. Ali *et al.*, Phys. Rev. D **55**, 4105 (1997).
[26] G. Buchalla and G. Isidori, Nucl. Phys. **B525**, 333 (1998).
[27] G. Buchalla, G. Isidori, and S.J. Rey, Nucl. Phys. **B511**, 594 (1998).
[28] A. Ali, T. Mannel, and T. Morozumi, Phys. Lett. B **273**, 505 (1991).

[29] F. Krüger and L.M. Sehgal, Phys. Lett. B **380**, 199 (1996).
[30] D. Melikhov, N. Nikitin, and S. Simula, Phys. Rev. D **57**, 6814 (1998).
[31] Z. Ligeti, I.W. Stewart, and M.B. Wise, Phys. Lett. B **420**, 359 (1998).
[32] A. Ali and G. Hiller, Phys. Rev. D **60**, 034017 (1999).
[33] CLEO Collaboration, S. Glenn, *et al.* Phys. Rev. Lett. **80**, 2289 (1998).
[34] CDF Collaboration, T. Affolder *et al.*, Phys. Rev. Lett. **83**, 3378 (1999).
[35] CLEO Collaboration, R. Godang *et al.*, Report CONF 98-22.
[36] N. G. Deshpande, J. Trampetic, and K. Panose, Phys. Rev. D **39**, 1461 (1989); C.S. Lim, T. Morozumi, and A.I. Sanda, Phys. Lett. B **218**, 343 (1989).
[37] C.A. Dominguez, N. Paver, and Riazuddin, Z. Phys. C **48**, 55 (1990).
[38] A. Ali and T. Mannel, Phys. Lett. B **264**, 447 (1991); **274**, 526(E) (1992).
[39] C. Greub, A. Ioannisian, and D. Wyler, Phys. Lett. B **346**, 149 (1994).
[40] D. Melikhov, N. Nikitin, and S. Simula, Phys. Lett. B **410**, 290 (1997); D. Melikhov and N. Nikitin, hep-ph/9609503.
[41] W. Roberts, Phys. Rev. D **54**, 863 (1996).
[42] C.Q. Geng and C.P. Kao, Phys. Rev. D **54**, 5636 (1996).
[43] P. Colangelo *et al.*, Phys. Rev. D **53**, 3672 (1996); **57**, 3186(E) (1998).
[44] G. Burdman, Phys. Rev. D **57**, 4254 (1998).
[45] I.I. Balitsky, V.M. Braun, and A.V. Kolesnichenko, Nucl. Phys. **B312**, 509 (1989).
[46] V.L. Chernyak and I.R. Zhitnitsky, Nucl. Phys. **B345**, 137 (1990).
[47] V.M. Braun, NORDITA-98-1-P (hep-ph/9801222).
[48] A. Khodjamirian and R. Rückl, WUE-ITP-97-049 (hep-ph/9801443).
[49] P. Ball and V.M. Braun, Phys. Rev. D **58**, 094016 (1998).
[50] P. Ball *et al.*, Nucl. Phys. **B529**, 323 (1998).
[51] P. Ball and V.M. Braun, Nucl. Phys. **B543**, 201 (1999).
[52] P. Ball, J. High Energy Phys. **09**, 005 (1998).
[53] P. Ball, J. High Energy Phys. **01**, 010 (1999).
[54] A.J. Buras and M. Münz, Phys. Rev. D **52**, 186 (1995).
[55] M. Misiak, Nucl. Phys. **B393**, 23 (1993); **B439**, 461(E) (1995).
[56] K. Chetyrkin, M. Misiak, and M. Münz, Phys. Lett. B **400**, 206 (1997); **425**, 425(E) (1998).
[57] ALEPH Collaboration, J. Nielsen, hep-ex/9908016.
[58] J. Charles *et al.*, Phys. Rev. D **60**, 014001 (1999).
[59] A.J. Buras *et al.*, Nucl. Phys. **B424**, 374 (1994).
[60] M. Jeżabek and J.H. Kühn, Nucl. Phys. **B320**, 20 (1989).
[61] M. Neubert and B. Stech, in *Heavy Flavors*, 2nd ed., edited by A.J. Buras and M. Lindner (World Scientific, Singapore, 1998).
[62] Z. Ligeti and M.B. Wise, Phys. Rev. D **53**, 4937 (1996).
[63] M. Bauer, B. Stech, and M. Wirbel, Z. Phys. C **34**, 103 (1987).
[64] T.E. Browder and K. Honscheid, Prog. Part. Nucl. Phys. **35**, 81 (1995).
[65] M.A. Shifman, A.I. Vainshtein, and V.I. Zakharov, Nucl. Phys. **B147**, 385 (1979); **B147**, 448 (1979); **B147**, 519 (1979).
[66] S.J. Brodsky and G.P. Lepage, in *Perturbative Quantum Chromodynamics*, edited by by A.H. Mueller (World Scientific, Singapore, 1989), p. 93; V.L. Chernyak and A.R. Zhitnitsky Pis'ma Zh. Éksp. Teor. Fiz. **25**, 544 (1977) [JETP Lett. **25**, 510 (1977)]; Yad. Fiz. **31**, 1053 (1980) [Sov. J. Nucl. Phys. **31**, 544 (1980)]; A.V. Efremov and A.V. Radyushkin, Phys. Lett. **94B**, 245 (1980); Teor. Mat. Fiz. **42**, 147 (1980); G.P. Lepage and S.J. Brodsky, Phys. Lett. **87B**, 359 (1979); Phys. Rev. D **22**, 2157 (1980); V.L. Chernyak, V.G. Serbo, and A.R. Zhitnitsky, Pis'ma Zh. Éksp. Teor. Fiz. **26**, 760 (1977) [JETP Lett. **26**, 594 (1977)]; Yad. Fiz. **31**, 1069 (1980) [Sov. J. Nucl. Phys. **31**, 552 (1980)].
[67] J.M. Flynn, talk given at the 7th International Symposium on Heavy Flavor Physics, Santa Barbara, CA, 1997, SHEP-97-25, hep-lat/9710080; H. Wittig, Lectures given at International School of Physics, ''Enrico Fermi,'' Varenna, Italy, 1997, OUTP-97-59-P, hep-lat/9710088.
[68] A. Ali, V.M. Braun, and H. Simma, Z. Phys. C **63**, 437 (1994).
[69] E. Bagan, P. Ball, and V.M. Braun, Phys. Lett. B **417**, 154 (1998).
[70] CLEO Collaboration, R. Ammar *et al.*, Phys. Rev. Lett. **71**, 674 (1993).
[71] A. Ali and C. Greub, Phys. Rev. D **57**, 2996 (1998).
[72] See, for example, F.M. Borzumati and C. Greub, Report PM-98-23 (1998), hep-ph/9810240.
[73] L.J. Hall, V.A. Kostelecky, and S. Raby, Nucl. Phys. **B267**, 415 (1986).